Seasonal and spatial pattern of dissolved organic matter bio- and photodegradation in boreal humic waters

Artem V. Chupakov[1], Natalia V. Neverova[1], Anna A. Chupakova[1], Svetlana A. Zabelina[1],

Liudmila S. Shirokova[1,2], Taissia Ya. Vorobyeva[1], Oleg S. Pokrovsky[2,3]*

[1] Institute of Ecological Problems of the North, N. Laverov Federal Center for Integrated Arctic Research, Nab Severnoi Dviny 23, Arkhangelsk 163000, Russia
[2] Geoscience and Environment Toulouse, UMR 5563 CNRS, University of Toulouse, 14 Avenue Edouard Belin, Toulouse 31400, France
[3] BIO-GEO-CLIM Laboratory, Tomsk State University, 35 Lenina Pr., Tomsk 634050, Russia

*corresponding author email: oleg.pokrovsky@get.omp.eu

Key words: bog, lake, stream, organic matter, metal, bacteria, sunlight

Synopsis:

In boreal humic waters of a forest lake and a bog, the rate of dissolved organic matter photodegradation is four times higher than that of biodegradation. However, given the shallow (0.5 m) light-penetrating layer, the biodegradation provides the largest contribution to CO_2 emission from water surfaces. A few trace metals were partially removed (1-10 %) during photo- and biodegradation, via precipitation of Fe(III) hydroxides after destabilization of organo-ferric colloids and organic complexes

Submitted to *Biogeosciences,* after *2nd* revision August 2024

Abstract

Studying competitive effects of microbial and light-induced degradation of dissolved organic matter (DOM) and trace metals is crucially important for understanding the factors controlling aquatic carbon (C), micronutrients and toxicants transformation in boreal waters. Here we characterized the degree of DOM and related major and trace element transformation under biotic activity and sunlight using conventional incubations of humic surface waters from the European subarctic: an ombrotrophic peatbog continuum (subsurface water – peatland pool – stream) and a stratified forest lake across seasons. Along the bog water continuum, biodegradation rate was the highest in subsurface waters collected via piezometer and the lowest in the acidic peatland pool. Photodegradation was similar for piezometrically collected subsurface waters and the stream, but was not detectable in the peatland pool. The waters of forest lake exhibited a strong seasonal effect of biodegradation, which was the highest in October and the lowest in June. Overall, the biodegradation was capable of removing between 1 and 7 % of initial DOC, being the highest in the forest lake in October and in peatland pool in summer. The photolysis was capable of degrading a much higher proportion of the initial DOC (10-25 %), especially in the forest lake during June and the bog stream during July. Only a few trace metals (TM) were sizably affected by both photo- and biodegradation of DOM (Fe, Al, Ti, Nb and light REE), whereas V, Mn, Co, Cu and Ba were affected solely by biodegradation. A likely mechanism of metal removal was their coprecipitation with coagulating Fe(III) hydroxides. Compared to typical CO_2 emissions from inland waters of the region, biodegradation of DOM can provide the totality of $C-CO_2$ evasion from lake water surfaces whereas bio- and photodegradation are not sufficient to explain the observed fluxes in bog water continuum. Overall, these results demonstrated strong spatial and seasonal variability in bio- and photodegradation of DOM and organic TM complexes, and call for the need of a systematic assessment of both processes across seasons with high spatial resolution.

1. Introduction

Organic Carbon (OC) processing via metabolic biological (heterotrophic bacteria uptake and respiration) and inorganic physico-chemical (photolysis) pathways is considered to be one of the major source of CO_2 supersaturation in surface waters and related C emissions (Lapierre et al., 2013; Tranvik et al., 2009), although the relative role of dissolved vs particulate organic carbon (DOC and POC, respectively) remains poorly quantified (e.g. Attermeyer et al., 2018; Lau et al., 2021; Shirokova et al., 2021; Keskitalo et al., 2022; Raudina et al., 2022). Given sizable CO_2 emissions in boreal and subarctic waters (Karlsson et al., 2021), together with high concentrations of DOC (Cole et al., 2007; Vonk et al., 2015), and fast ongoing and predicted environmental changes in high latitude aquatic and terrestrial ecosystems (Wauthy et al., 2018; Chaudhary et al., 2020; Harris et al., 2022), the surface waters of subarctic regions are at the forefront of studies on the biogeochemical cycle of C. Although emissions from these waters are significantly lower than those in the 10 °S – 10 °N equatorial belt (e.g., Borges et al., 2015), the magnitude of possible changes in C flux from northern waters to the atmosphere remains much less known. Further, there are still important geographical biases linked to insufficient knowledge of rates and mechanisms of DOC transformation in certain regions. An example is wetland-dominated northern aquatic settings, where high concentrations of soil organic C surrounding the bogs provide high concentrations of DOC but also some related trace metals, whose concentration and migration can be strongly controlled by processes of dissolved organic matter (DOM) transformaion.

Thorough laboratory and field work on DOM bio- and photolability conducted over the past decades have demonstrated both phenomena are important, and, depending on environmental setting (nutrient regime, photic layer depth, nature of DOM, etc.), one or another may dominate overall DOM removal in surface waters (Vachon et al., 2016, 2017; Vähätalo and Wetzel, 2008; Obernosterer and Benner, 2004). In addition to DOM, trace elements (limiting

micronutrients, toxicants and geochemical tracers) present in the form of organic and organo-mineral (Fe, Al) colloids and organic matter comlexes may be subjected to strong transformations during microbioological and photoltic degradations of DOM. This in turn may impact the bioavailability, toxicity and export fluxes of trace metals in from terrestrial to aquatic continental and finally coastal environments.

Recently, specific attention was devoted to the aquatic systems of permafrost peatlands given their high vulnerability to climate warming and huge potential for release of soil organic C to surfaces waters (Vonk et al., 2015; Shirokova et al., 2019; Payandi-Rolland et al., 2020; Prijac et al., 2022; Rosset et al., 2022; Taillardet et al., 2022). These studies provided a range of DOM susceptibility to biotic degradation. Thus, between 10 and 40 % of the DOC in lakes, rivers and soil waters of the boreal zone may be available for bacterial uptake over a time frame of several weeks (Berggren et al., 2010; Roehm et al., 2009). This range is consistent with 14-16% of biodegradable DOC (BDOC) assessed globally (Begum et al. 2022). The necessity for further studies was also indicated, most notably with regard to *i*) seasonal aspects, given that the overwhelming majority of available studies were performed during Arctic summer (see discussions in Vonk et al., 2015; Laurion et al., 2021), and *ii*) increased spatial resolution, given that sizable variations of BDOC can be observed within quite short distances of a hydrological continuum (Payandi-Rolland et al., 2020; Raudina et al., 2022). Another poorly studied aspect is DOM photo- and biolability across the depth of the water column, especially in seasonally stratified lakes which are subject to spring and autumn overturn.

Based on a compilation of available studies on BDOC and their own research, Vonk et al. (2015) argued there is a negligible amount of biodegradable DOC in aquatic systems without permafrost. This is, however, contradictory to available assessments on biodegradation of aquatic DOM as major driver of CO_2 emission in general (Amaral et al., 2021; Liu and Wang, 2022) and in boreal waters in particular (Ask et al., 2012; Lapierre et al., 2013). Furthermore, among all

Arctic rivers, the highest annual (20%) and winter (ca. 45%) biodegradable DOC (BDOC) was reported for the Ob River, which drains through peatlands with minimal permafrost influence (Wickland et al., 2012). These non-exhaustive examples illustrate certain inconsistency in current estimations of DOC biodegradability in surface organic-rich waters of high latitudes, which precludes quantitative modeling of future C fluxes between land, water and atmosphere in these environmentally important regions. Towards addressing these inconsistences, in this study, we chose a typical hydrological continuum in a boreal ombrotrophic bog in a glacial lake-ridge complex that includes subsurface water, a small peatland pool in the central part of the bog and an outlet stream. Further, we selected a well-studied deep stratified humic lake in the same region (Lake Temnoe; Chupakov et al., 2017) where we sampled surface and deep horizons for the incubation experiments. The chosen waters represent subarctic non-permafrost regions that exhibit sizable organic C pool in their soils and high concentrations of DOC in their surface waters. In contrast to previous studies of permafrost peatlands (Shirokova et al., 2019; Laurion et al., 2021; Payandi-Rolland et al., 2020; Mazoyer et al., 2022) where the main source of DOM is peat or ground vegetation like mosses and lichens, in this highly productive southern taiga region, DOC may be more vulnerable to microbial activity due to the presence of forest leachates (i.e., Don and Kalbitz, 2005; Kalbitz et al., 2003; Kawahigashi et al., 2004; Kiikkilä et al., 2013) and much higher bioproductivity for both the terrestrial and aquatic parts of the lake-river ecosystems. A broad importance of DOM bio- and photodegradation dynamics is that these processes can contribute to CO_2 emissions from water surfaces thereby directly controlling the C cycling between the land and the atmopshere.

The first working hypothesis behind our study design is that the DOC-rich subsurface water and deep horizons of the humic lake are mostly sensitive to sunlight impact (Stubbins et al., 2010), and that maximal impact of photodegradation is expected during allochthonous aromatic DOM input (high surface inflow to lakes and bogs in June and October). In contrast,

maximal biodegradation of DOM is expected during periods of possible phytoplankton bloom in August, when autochthonous organic material is generated in the water column. An important novelty of the present study is adressing trace metal (TM) partitioning during bio- and photodegradation. The link between DOM and TE is straightforward: in humic waters of peatlands, most TE (except probably some alkalis and oxyanions) are strongly ($> 80\%$) associated to DOM in the form of organic and organo-mineral (Fe, Al) colloids (Pokrovsky et al., 2005, 2012, 2016). As a result, any DOM transformation processes may directly control the pattern of TE. From the other hand, some TE may be photosensitive (Mn, Fe), toxic (Al, Cu, As, Cd, Pb), or limiting micronutrients (Zn, Co, Ni, Mo) for the bacteria. Our second working hypothesis here is that removal of DOM via photo- or bio-degradation will change the partitioning of trace elements which are either *i*) strongly bound to DOM, such as divalent transition metals, or *ii*) incorporated into organo-mineral (Fe, Al) colloids, such as trivalent and tetravalent hydorlysates. The TE of 1st group might either remain in solution (during photodegradation), hence not modifying their total dissolved concentration, or being taken up by growing bacteria during bio-degradation of TE-bound organic matter (Shirokova et al., 2017a, c). The elements of the second group are capable of co-precipitating with Fe and Al hydroxides hence being scanvenged from the aqueous solution.(e.g., Kopacek et al., 2005, 2006). To test these hypotheses, we examined DOM and related trace metals bio- and photodegradability aiming to assess 1) spatial variations along a hydrological continuum of non-permafrost peatland and different horizons of a neighboring deep stratified lake located in the forest, and 2) temporal variability during 3 main hydrological seasons (high flow in June, baseflow in August and autumn rain season in October) in the forest lake. Achieving these objectives should allow quantifying the relative share of bio- and photodegradation on overall DOC and TM removal from surface waters via biotic and physico-chemical mechanisms. The third aim of this study

 was to relate the measured rates of DOM photo and biodegradation to CO_2 emissions observed

 in the studied water bodies.

159

160 **2. Materials and Methods**

161   *2.1. Natural settings of subarctic bog and stratified lake*

162   The study site is in the NE part of the European boreal zone (Arkhangelsk region), **Fig.**

163 **1**. The mean annual air temperature is 0 °C and average annual precipitation is 700 ± 50 mm.

164 The pristine ombrotrophic Ilasskoe Bog is located 30 km SE of Arkhangelsk, and is a typical

165 lake-ridge complex formed from the last glaciation approximately 10,000 years ago. Its total

166 surface area is 89 km², with an average peat thickness of 3 m. The hydrological continuum of the

167 Ilasskoe Bog includes subsurface water collected via piezometer (2-2.5 m depth), a small lake

168 (Severnoe) and a stream outlet (**Fig. 1**). Lake Severnoe, located in the central part of the bog, is

169 a typical peatland pool with an average depth of 1.5 m and a surface area of 0.013 km². The

170 Chernyi Stream is an outlet for the eastern part of the bog. The stream is 0.7-2.0 m wide, 10 km

171 long and it flows in a forested (taiga) zone in the shade of tree canopy. The waters of the Ilasskoe

172 Bog are acidic (pH ranges from 3.9-4.0 in piezometer and peatland pool to 5.7 in stream Chernyi),

173 organic-rich (DOC is equal to 88, 13 and 38 mg L^{-1} in the piezometer, lake and stream,

174 accordingly) and low mineralized (Electrical Conductivity is 17-46 µS cm^{-1}), as listed in **Table**

175 **1**.

176   Lake Temnoe is located in a pristine forest 100 km NNE of the town of Arkhangelsk, an

177 area that does not receive any direct anthropogenic impact (**Fig. 1**). The watershed area is 3.08

178 km² and the lake surface area is 0.091 km², with a maximum depth of 37 m and a Secchi disk

179 depth of 3.5±0.5 m. The water residence time in the lake is 394 days. Bogs constitute 31% of

180 lake's watershed area, which is represented by carbonate-free loamy moraine atop the peat,

181 podzol and gley soils. The lake water is slightly acidic (pH = 5.1 to 6.0), humic (DOC = 13-20

182 mg L^{-1}) and dominated by allochthonous DOM with a low concentration of total dissolved ions

183 (Electrical Conductivity of 20 µS cm^{-1}). Similar to other deep boreal and subarctic lakes, the lake

184 exhibits 2 main periods of pronounced stratification (November to April and June to September)

185 and two periods of lake overturn (October and May). Maximal winter stratification occurs in

186 March; the highest water temperature typically occurs in July (see Chupakov et al., 2017 for

187 details).

188   The surface waters were collected from the shore (peatland pool and stream) or a PVC

189 boat (Lake Temnoe). Surface (30-50 cm depth) waters were sampled in the Ilasskoe bog and 3

190 water horizons (0.5, 5 and 10 m) were sampled in the Temnoe Lake using a pre-cleaned

191 polycarbonate horizontal water sampler (Aquatic Research Co, ID, USA). The water samples

192 were placed into 2-L Milli-Q pre-cleaned PVC jars and kept refrigerated (4 °C) until arrival at

193 the laboratory within 2-3 hours of collection.

194

195   *2.2. Experiments*

196   2.2.1. Biodegradation

197   For DOM biodegradation assessments we followed the recommended protocol and used

198 the appropriate type of labware for assessing biodegradable DOC of Arctic waters without

199 external nutrient addition (Vonk et al., 2015; Payandi-Rolland et al., 2020) and applied a slight

200 modification from Shirokova et al. (2019) to assess maximal possible biodegradation. Initial

201 water samples brought to the laboratory within 2-3 hours after sampling were filtered through 3

202 µm sterilized Nylon Sartorius membranes (47 mm diameter); these were used because

203 'conventional' 0.8-1.2 µm (GF/F) filtration membranes might remove too many microbial cells

204 (Dean et al., 2018).

205   Duplicate 30 mL aliquots of 3 µm-filtered water were placed into pre-combusted (4.5

206 hours at 450°C) dark borosilicate 40 mL glass bottles wrapped in Al foil to prevent any

photolysis, without nutrient amendment and incubated at $22\pm1°C$ in the dark. The bottles were

closed with loosened sterilized PVC caps to allow air exchange. The bottles were shaken

manually once a day avoiding the liquid touching the cap. The entire reactor was used for

sampling after 0, 2, 5, 8, 12, and 21 days of exposure. Sampled solutions were filtered through

sterile, MilliQ-cleaned Sartorius 0.22 µm filters. The DOC blanks for these filters did not exceed

1% of DOC concentrations in experimental samples. Sterilized control reactors were filled with

natural water that was filtered through a 0.22 µm sterile filter and incubated together with

experimental reactors following the approach of Köhler et al (2002).

All handling and sampling of bottles was performed in the laminar hood box in a sterilized

workspace. Filtered samples were acidified with 30 µL of concentrated (8.1 M) double distilled

HCl, tightly capped and stored in the refrigerator before DOC analyses. The non-acidified portion

of filtrate was used for pH, Specific Conductivity, DIC and $UV_{254\ nm}$ and optical spectra

measurement. Control runs were 0.22 µm sterile-filtered water which was incubated in parallel

with experiments and re-filtered through 0.22 µm filters the day of sampling. To ensure

minimized release from sterilized Nylon membrane, we ran blank (Milli-Q) filtrations through

both GF/F and 0.22 µm Nylon filters; in both cases the DOC blank was below 0.1-0.2 mg/L

which is less than 1% of DOC concentration in our samples. The glass bottles were incubated in

duplicates at $22\pm1°C$ and agitated manually at least once a day over the 16 days of exposure.

2.2.2. Photodegradation

For photodegradation incubations, water samples were collected in Al-foil covered pre-

cleaned polypropylene jars and sterile filtered (0.22 µm Nalgene Rapid-Flow Sterile Systems)

within 2 hours of sampling and refrigerated. The filtrates were transferred under laminar hood

box into sterilized, acid-washed quartz tubes (150 mL volume, 20% air headspace) with silicate

stoppers and placed at 3 ± 2 cm depth into an outdoor pool which was filled by river water having

232 the light transparency similar to that of the Ilasskoe and Temnoe lakes. The outdoor pools were

233 placed in an unshaded area with a latitude similar to the sampling sites (< 30 km from Ilasskoe

234 Bog and Temnoe Lake). Slight wind movement and regular manual shaking allowed for

235 sufficient mixing of reactor interiors during exposure. All photodegradation experiments were

236 run in duplicates. The water temperature (EBRO EBI 20) and light intensity (Luxmeter Testo

237 545) were continuously recorded every 3 hours.

238   For DOM photodegradation experiments, we followed conventional methods requiring

239 exposure of 0.2 µm-sterile filtered samples in quartz reactors in the outdoor pool (Vähätalo et

240 al., 2003; Chupakova et al., 2018; Gareis and Lesack, 2018), solar simulator (Lou and Xie, 2006;

241 Amado et al., 2014) or directly in the lake water (Laurion and Mladenov, 2013; Groeneveld et

242 al., 2016). Note that the 0.22 µm sterile filtration is the only way of conducting photodegradation

243 experiments, given that autoclave sterilization of DOM-rich natural waters would coagulate

244 humic material and thereby would not be suitable (Andersson et al., 2018). Filtration through a

245 smaller pore size, however, would decrease the concentration of DOC and trace metals (i.e., Ilina

246 et al., 2014; Vasyukova et al., 2010). We have chosen a 16 day exposure time for logistical

247 constraints, which is still consistent with biodegradation experiments described above and with

248 the duration used in previous studies on photodegradation under sunlight, from 15 to 70 days

249 (Moran et al., 2000; Vähätalo and Wetzel, 2004; Mostofa et al., 2007; Chupakova et al., 2018).

250 Dark control experiments were conducted also in duplicates, using sterilized glass tubes filled

251 with sterile 0.22 µm-filtered water, wrapped in Al foil and placed in the same outdoor pool as

252 the experiments. The headspace (approx. 20% of total reaction volume) was similar in

253 experimental and control reactors. The individual reactors were sterile sampled at the beginning

254 and after the 0, 2, 5, 8, 12, and 16 days of exposure. Each sampling sacrificed the entire reactor.

255 The Milli-Q blanks were collected and processed to monitor for any potential sample

256   contamination introduced by our filtration, incubation, handling and sampling procedures. The

257   organic carbon blanks of the filtrates did not exceed 0.2 mg/L.

258

259   *2.3. Analyses*

260   The temperature, pH, O_2 and specific conductivity in surface waters were measured in

261   the field. The dissolved CO_2 concentration in the studied bodies of water was measured in-situ

262   using submersible Vaissala Carbocap® GM70 handheld carbon dioxide meter with GMP222

263   probes (accuracy 1.5%; see Serikova et al. (2018, 2019) for methodological details). The

264   diffusional CO_2 flux was calculated using a wind-based model (Cole and Caraco, 1998) with k_{600}

265    $=2.07+0.215 \times u_{10}^{1.7}$, where u_{10} is the wind speed at 10 m height, following the approaches

266   developed for surface waters of peatlands (Zabelina et al., 2021).

267   The DOC and DIC were analyzed by high-temperature catalytic oxidation using a

268   Shimadzu® TOC-VCSN (uncertainty $\pm 2\%$, 0.1 mg L^{-1} detection limit). DIC was measured after

269   sample acidification with HCl and DOC was analyzed in acidified samples after sparging it with

270   C-free air for 3 min at 100 mL min^{-1} as non-purgable organic carbon (NPOC). Internationally

271   certified water samples (MISSISSIPPI-03 and Pérade-20) were used to check validity and

272   reproducibility of the analysis. Filtered sampled collected from photodegradation experiments

273   were acidified with ultrapure nitric acid and analyzed for major and TE following the procedures

274   employed by Geoscience and Environment Toulouse Laboratory for analyses of boreal humic

275   waters (Oleinikova et al., 2017, 2018).

276   The UV- and visual absorbance of water samples was measured using a 10 mm quartz

277   cuvette on a CARY-50 UV-vis spectrophotometer to assess the aromaticity of pore fluids via

278   specific UV absorbance ($SUVA_{254}$). In the filtrates, we measured optical density at 254 nm and

279   at selected wavelengths (365, 436, 470, and 665 nm) as well as the entire UV-visible spectrum.

280   The specific UV-absorbency ($SUVA_{254}$, L mg^{-1} m^{-1}) and $E_{470}:E_{665}$ ratios are used as a proxy for

degree of condensation of aromatic groups of DOM, or humification (Chin et al., 1994; Weishaar et al., 2003; Hur et al., 2006; Peacock et al., 2013). The ratio $E_{254}:E_{436}$ is useful for evaluation of contributions of autochtonous (aquatic) DOM compared to terrestrial (soil) C (Hur et al., 2006; Ilina et al., 2014). The ratio $E_{254}:E_{365}$ also allows approximating the mean molecular weight of DOM (Hiriart-Baer et al., 2008; Berggren et al., 2007). For better visualization of the differences in spectral parameters between experimental and control reactors, we calculated the difference (ΔA) between the absorbance of the photo- or bio-reactor and that of the control reactor at each sampling time.

Major cations, Si, P and ~40 TE were measured with a quadrupole ICP-MS (Agilent 7500 ce) using In and Re as internal standards. The international geo-standard SLRS-6 (Riverine Water Reference Material for Trace Metals) was used to check validity and reproducibility of analyses. Note that for both bio- and photodegradation experiments, ICP MS analyses were performed over 16 days of incubation time.

To check for possible microbial development in biodegradation experiments, we performed oligotrophic and eutrophic bacteria counts over the course of incubation, following the standard methodology used in biodegradation experiments of peat waters (Stutter et al., 2013) and also described previously (Shirokova et al., 2017b; Chupakova et al., 2018). Specifically, active bacteria number count (colony forming units, CFU mL^{-1}) was performed using Petri dishes inoculation (0.1 to 1.0 mL of lake water in three replicates) performed in a laminar hood box immediately prior the experimental incubation start and upon each sampling. Samples were inoculated on Nutrient Agar (5 g L^{-1} beef extract, 5 g L^{-1} gelatine peptone, 15 g L^{-1} bacteriological agar, pH=6.8±0.2 at 25 °C) to determine the total number of heterotrophic bacteria. Difco@ agar (granulated powder, Lot No 6290083) inoculation was used to assess the number of oligotrophic bacteria. Inoculation of blanks was routinely performed to assure the absence of contamination from external environments.

2.4. Data treatment

The bio- and photodegradable DOC and trace metals were calculated as percent loss relative to control in similar fashion with other studies (Vonk et al., 2015; Chupakova et al., 2018; Shirokova et al., 2017b, 2019). However, previous works in similar environmental contexts of high-DOC humic waters demonstrated that the effects of DOC and element decrease are rather low and often comparable to uncertainties of duplicates (Shirokova et al., 2019). To assess the net effect of bio- or photodestruction during the experiment, we used the integral values of concentration change, estimated as the difference between the experiment and the control, while taking into account the standard deviation of replicates. For this, we first calculated the mean of replicates at the i-th time of sampling for the experiment and the control of X component ($^{mean}X_i$ and $^{control}X_i$, respectively). We next calculated the sum of mean concentration of replicates and its standard deviation ($^{mean}X_i + SD_i$). Thus, we obtained 3 values characterizing the bio- or photo-degradation process: 1) the change of concentration in the experimental reactor (^{mean}S), 2) the change of concentration not linked to the studied process ($^{control}S$), and 3) the maximal uncertainty of the concentration change in the reactor ($^{mean+SD}S$). This allowed calculating, in percentages, the efficiency of bio or photodegradation of X component relative to the control, taken into account relevant uncertainties as following:

$$X\,(\%) = 100 \times (|^{mean}X| - |^{control}X|)/|^{control}X| \qquad (1)$$

$$SD\,(\%) = 100 \times (|^{mean+SD}X| - |^{mean}X|)/|^{control}X| \qquad (2)$$

where X is biodegradable DOC or trace element (BDOC and BTE, respectively) or photodegradable DOC and trace element (PDOC and PTE, respectively). The sign of X designates either a decrease («–») or an increase (« + ») of solute concentration during the experiment. We considered the decrease of concentration significant when $X\,(\%) > SD\,(\%)$. In other cases, the change was non-systematic over the course of experiment or non-measurable using the experimental technique employed in the present study.

331   The mean rate of bio- or photodegradation of X component (V_X) was calculated based on

332   the overall change (ΔX, in %) between the initial (X_0) and final value normalized to overall

333   duration of the experiment t (22 and 16 days for bio- and photodegradation, respectively):

334    $$V_X = ((\Delta X / X_0) / t \qquad\qquad (3)$$

335   The SD for rates of component change were calculated in a similar way.

336   The spectral differences between experimental and control reactors were presented as X-

337   Y-Z diagrams where X is elapsed time, Y is wavelength, and Z is ΔA. The data were plotted in

338   a Surfer software package using triangulation with a linear interpolation method. Statistical

339   treatment included the least squares method and the Pearson correlation, as the data were

340   normally distributed. All calculations were performed in STATISTICA ver. 10 (StatSoft

341   Inc.,Tulsa) at $p = 0.05$).

342

343   **3. Results**

344   *3.1. Field measured C concentration and calculated CO_2 fluxes*

345   The DOC concentration ([DOC]) ranged from 13 to 21 mg L^{-1} in Lake Temnoe,

346   depending on depth and season. The CO_2 concentrations and fluxes increased from June to

347   October and varied from 99 to 220 µmol L^{-1} and 32 to 71 mmol CO_2 m^{-2} d^{-1}, respectively (**Table**

348   **1**). In Ilasskoe Bog hydrological continuum, the DOC decreased from 88 mg L^{-1} in the peat soil

349   water to 38 mg L^{-1} in the outlet stream. The DOC concentration was generally similar (within ±

350   5 %) between 3, 0.8 (GFF), 0.45 and 0.22 µm pore size filtration of the initial sample, which is

351   in agreement with former size fractionation measurements for Arctic and subarctic systems

352   (Vasyukova et al., 2010; Pokrovsky et al., 2012, 2016, Shirokova et al., 2019). The waters of

353   Ilasskoe Bog continuum exhibited CO_2 supersaturation with respect to atmosphere (from 55 to

354   3300 µmol L^{-1}) and calculated CO_2 emission (diffusion) flux ranging from 22 mmol CO_2 m^{-2} d^{-1}

355   in the peatland pool to 1600 mmol CO_2 m^{-2} d^{-1} in the piezometer (**Table 1**).

 3.2. Biodegradation of DOM

357 3.2.1. DOC concentration evolution in the experiments

358   In the Temnoe Lake, the range of [DOC] change during 2-3 week incubation in the

359 experimental reactors did not exceed 2 mg L^{-1} and remained within +0.5 to -1.5 mg L^{-1}, which is

360 less than 10% of the initial DOC amount (**Fig. 2 A and Fig. S1** of the Supplement). The

361 biodegradable DOC was both season and depth dependent and ranged from 2 to 6 % (**Table 2**).

362 The integral 2-week rates of biodegradation (**Table 3, Fig. 3 A**) demonstrated the highest values

363 during autumn at depths of 0.5 m and 10 m and the lowest values during June at all depths. The

364 final 0-10 m water column- and season-averaged biodegradation rate in Lake Temnoe ranged

365 from 0.02 to 0.04 mg DOC L^{-1} d^{-1}. Integral rates of bio-degradation in the 0-10 m layer

366 demonstrated an increase from May to October, over the entire open-water period (**Fig. 4 A**).

367   For Ilasskoe Bog, the BDOC was highest in the peatland pool (4.9 ± 1.4 %) and lowest

368 in the outlet stream (3.1 ± 2.4 %; **Fig. 2 A** and **Fig. S1**). The integral rate of DOC biodegradation

369 followed the order 'piezometer >> stream > peatland pool' and ranged from 0.03 to 0.17 mg C

370 L^{-1} d^{-1} (**Table 3, Fig. 3 A**).

371

372 3.2.2. Optical parameters of DOM

373   In Lake Temnoe, the $SUVA_{254}$ remained relatively constant (4.2 to 4.6 L mg C^{-1} m^{-1})

374 across seasons and depths (**Table 1 B**). Over the course of biodegradation, the $SUVA_{254}$ did not

375 change significantly (i.e., less than 0.2 units, which is comparable to the variability of duplicates;

376 **Fig. S2**). The ratio $E_{254}:E_{436}$, which is an indicator of humification, increased with incubation

377 time in Lake Temnoe waters; the magnitude of this increase across depth followed the order "0.5

378 m > 5 m > 10 m" (**Fig. S3**). The ratio E_{254}/E_{365} also increased over the course of biodegradation,

379 corresponding to an increase of mean molecular weight of DOM (Hiriart-Baer et al., 2008;

380 Berggren et al., 2007). The ratio E_{365}/E_{470} also demonstrated the strongest increase in surface

horizons and virtually no change in the deepest horizon (**Fig. S3**). An increase in the ratio $E_{470}:E_{665}$ corresponds to a decrease in the degree of aromaticity (humification). An increase in the ratio $E_{254}:E_{436}$ signifies a decrease in contribution of autochthonous (aquatic) DOM compared to terrestrial (soil) C, whereas an increase in the $E_{254}:E_{365}$ ratio characterizes removal of low molecular weights compounds.

In Ilasskoe Bog samples, the highest SUVA was observed in the water of the piezometer and the lowest in the stream, but the evolution of this parameter in the course of biodegradation was rather weak (**Fig. S3**). The $E_{254}:E_{365}$ and $E_{254}:E_{436}$ ratios increased with incubation time in the piezometer and decreased with time in the stream (**Fig. S3**). The optical ratios ($E_{254}:E_{436}$, $E_{365}:E_{470}$, $E_{470}:E_{665}$) increased in the peatland pool, suggesting an increase in the molecular weight and an increase in the ratio of aromatic to aliphatic compounds.

Complete spectral differences between the experimental and control samples demonstrated rather weak ($\Delta A \leq 0.04$) changes of spectral parameters, mostly detectable after 10-12 days of incubation (**Fig. S4**). These results were generally consistent with the discrete spectral parameters presented above and demonstrated maximal effects in the piezometer and bog outlet stream. In Lake Temnoe, the maximal impact of biodegradation on spectral parameters was observed in June, at 0.5 m depth.

3.2.3. Bacterial number evolution during biodegradation experiments

The number of cultivable eutrophic bacteria (EB) sizably (ca., 2 orders of magnitude) increased during biodegradation of Lake Temnoe waters. However, this evolution was not systematic in the course of incubation; there was a pronounced decrease after 2 weeks of exposure in June and August and rather stable concentration in waters of all horizons sampled in October (**Fig. S5**). Such maxima in June and August might be linked to consumption of substrate/nutrient limitations on bacterial growth. In Ilasskoe Bog continuum, the number of

eutrophic bacteria decreased by an order of magnitude in the peatland pool and piezometer while it remained constant in the stream. The number of oligotrophic bacteria (OB) increased in waters of all Lake Temnoe horizons by ca. 2 orders of magnitude in August and October and 1 order of magnitude in June. In contrast, the OB number did not change or slightly decreased during incubations of waters from Ilasskoe Bog continuum (**Fig. S5**).

3.2.4 Trace element behavior

During biodegradation experiments, a number of trace metals [Group 1] demonstrated a significant ($X > SD$, Eqn. 1) decrease in concentration across the incubation period (**Table 2**): Al, Ti, Fe, Co, Cu, Ba, Nb, light REE (LREE) and Pb (as illustrated for Fe in **Fig. 5**) as well as Mn, V, and La (**Figs. S6, S7 and S8**, respectively). The most significant effects were observed for Fe in the 0-5 m horizon of Lake Temnoe (9 to 18 % in June, 6 to 13.5 % in August and 8 to 9.5 % in October) and 14% in the peatland pool of Ilasskoe Bog. Overall, for most elements except Fe and Mn, this increase was less pronounced than that of DOC; maximal effects were achieved for Lake Temnoe in August and October (V, Mn, Co, Cu, Ni, Nb, Hf, Pb and Th) and in June (Al and Ti). These elements are typically linked to DOM and Fe and present in the form of organic- and organo-mineral colloids. Second group of major and trace elements did not appreciably change their concentration (< 2 % decrease): Li, B, Na, Mg, K, Ca, Si, Ge, As, Rb, Sr, Mo, Sb, Mo and Ba. These elements are not linked to colloids of Fe(III) hydroxide and organic matter. Finally, some elements [Group 3] exhibited unstable behavior without systematic change in concentration during the exposure ($X < SD$, Eqns. 1-2): Cr, Zn, Cu, Sr, Cd, (Y, Zr), Cs, Tl and U. These elements cannot be considered as significantly impacted by the biodegradation process in Lake Temnoe water.

In the Ilasskoe Bog hydrological continuum, the most significant changes during biodegradation were observed in the peatland pool and outlet stream. Elements strongly (> 5-10

431 %; X > S.D. in Eqn. 1) affected by biodegradation were organically / colloidally comlexed V,

432 Fe, Ni, Ga, Y, LREEs and Pb.

433

434 *3.3. Photodegradation of DOM*

435 3.3.1. DOC concentration evolution

436 Compared to biodegradation, photodegradation demonstrated much higher values of

437 PDOC and rates of reaction as well as higher variability among seasons and sites. In Lake

438 Temnoe, the PDOC was the highest in June and the lowest in October (**Fig. 2 B** and **Table 2**).

439 The maximal range of concentration change during 2-week period achieved 6-8 mg L^{-1} (**Fig. S9**)

440 which was 10 to 20 % of the initial [DOC] values. The rates strongly decreased from May-June

441 to the end of summer – autumn. The depth integrated (0 to 10 m) rate of DOM photodegradation

442 in Lake Temnoe ranged from 0 in October to 0.2 mg C L^{-1} d^{-1} in June (**Table 3**; **Fig. 4 B**).

443 In the Ilasskoe Bog hydrological continuum during July, the photodegradation rate

444 followed the order "outlet stream > piezometer >> peatland pool" (**Fig. 3 B**), where integral rates

445 equaled to 0.27±0.04, 0.33±0.07, and 0±0.05 mg C L^{-1} d^{-1}, respectively (**Table 3**).

446

447 3.3.2. Optical parameters of DOM

448 Similar to the DOC concentration, the optical parameters of DOM more strongly evolved

449 over the course of photodegradation compared to the biodegradation experiments. In the Temnoe

450 Lake, the strongest decrease in SUVA$_{254}$ was observed in the waters of all horizons in June. This

451 decrease was less pronounced in October (**Fig. S10**). The E$_{254}$:E$_{365}$ ratio demonstrated a sizable

452 increase in June, with much weaker increase in October. The E$_{254}$:E$_{436}$ ratio strongly decreased

453 with exposure time throughout all seasons (10 m depth) and only in June in the surface horizons

454 (**Fig. S11**). An increase in the ratio E$_{254}$:E$_{365}$ over the course of photodegradation corresponded

455 to an increase in mean molecular weight of DOM. The ratios E$_{365}$:E$_{470}$ and E$_{470}$:E$_{665}$ decreased

in all experiments with the Temnoe Lake waters (**Fig. S11**), suggesting a decrease in the degree

of humification (Battin, 1998) and a decrease in the ratio of aromatic to aliphatic moieties.

The SUVA$_{254}$ in Ilasskoe Bog waters remained stable during photodegradation of stream

waters and piezometer and strongly decreased in the peatland pool (**Fig. S10**). The E$_{254}$:E$_{436}$ ratio

strongly increased in the peatland pool and exhibited a decrease in stream waters and piezometer,

whereas the E$_{365}$:E$_{470}$ ratio systematically decreased in all photodegradation experiments with

the Ilasskoe Bog continuum (**Fig. S11**). Finally, the E$_{470}$:E$_{665}$ ratio exhibited sizable decrease, in

the order 'stream >> pool ≥ piezometer'. The total spectral differences between experimental and

control reactors were mostly pronounced in stratified forest lake waters in June (ΔA = -0.4 to -

0.4) and in the bog continuum in July, where effects were strongest in the piezometer and outlet

stream waters (ΔA parameter as high as – 0.4 (**Fig. S12**).

3.3.3. TE in photodegradation experiments

The elements affected by photodegradation also formed three groups similar to those

impacted by biodegradation. Concentrations of Al, Fe, trivalent and tetravalent hydrolysates (Ti,

Ga, Zr, Y, LREE and Th) and Nb of [Group 1] significantly (> 2 %; $p < 0.05$) decreased during

photolysis as illustrated for Fe in **Fig. 6,** and for Ti and Zr in **Figs. S13** and **S14,** respectively.

The decrease of Fe was mostly pronounced in Lake Temnoe water from 10 m depth, whereas

that of Ti and Zr was detectable for all horizons and seasons except in October. For the Ilasskoe

Bog continuum, there was no systematic change in Fe concentration, whereas concentrations of

Ti and Zr systematically decreased over the course of sunlight exposure (**Figs. S13, S14**). Alkali

(Li, Rb), alkaline-earth metals (Mg, Ca, Sr, Ba), Si and oxyanions (As, Mo, Sb) of [Group 2]

were weakly (< 2 %) affected by photolysis. Finally, the remaining trace elements of [Group 3]

did not exhibit any systematic evolution of concentration during exposure to sunlight, or these

changes were inferior to the uncertainties of replicates (X < S.D. in Eqn. 1).

481   We found that, unlike for DOC, the magnitude of trace element concentration decrease

482   during photodegradation was generally lower than that of biodegradation experiments. Overall,

483   the strongest effects were observed for Ti (3 to 9% in Lake Temnoe; 20% in Ilasskoe Bog), Ga

484   (6 to 14%), Zr (14-17% in Lake Temnoe), Nb (8 to 13%) and Th (8 to 19% in the Temnoe Lake

485   and up to 50% in the Ilasskoe Bog). These effects were mostly pronounced in the Temnoe Lake

486   in June and August and in peatland pool of the Ilasskoe Bog (July).

487

488   **4. Discussion**

489   *4.1. Comparison between biodegradation and photolysis*

490   The impact of season on the biodegradable DOC could be tested only for Lake Temnoe

491   because it was sampled during the 3 main hydrological periods. The maximal biodegradation of

492   the lake water was observed during autumn, when large amount of labile fresh soil OM and plant

493   litter were delivered to the lake from the watershed via surface runoff. The water temperature

494   seems to be of secondary importance for the intensity and rate of DOM biodegradation. This is

495   also confirmed by lack of statistically significant (at $p < 0.05$) correlation between water

496   temperature and BDOC parameters (overall magnitude and rate). It is worth noting that the

497   seasonal pattern of BDOC in the humic lake quantified in this study (**Fig. 4 A**) contrasted with

498   previous works on biodegradation of large Arctic streams and rivers whose BDOC decreased as

499   the Arctic summer progressed (Vonk et al., 2015). Presumably, the input of fresh plant litter from

500   the forested watershed of Lake Temnoe provided elevated biodegradation in the water column at

501   the end of the open water season. Another reason could be due to lake overturn in October and

502   exposure of deep, partially autochthonous, and thus biodegradable, DOM to the surface horizons.

503   A supply of limiting nutrients (N and P) to the upper 0-10 m layer during lake overturn could

504   also promote such biodegradation in October.

The highest biodegradation rates in the uppermost sections of the bog hydrological continuum (piezometer, **Fig. 3 A**) are consistent with recent findings on organic-rich waters of permafrost peatlands (Shirokova et al., 2019; Payandi-Rolland et al., 2020) and earlier results on headwaters, small streams and soil leachates (Roehm et al., 2009; Ilina et al., 2014; Mann et al., 2014, 2015; Larouche et al., 2015; Spencer et al., 2015; Vonk et al., 2015; Moody et al., 2013; Pickard et al., 2017; Dean et al., 2019). This could be due to the very short water residence time and freshly leached DOM in these water objects (i.e., Mann et al., 2012; Abbott et al., 2014; Payandi-Rolland et al., 2020), given that bioavailable DOM components leached from plant litter are rapidly utilized (Textor et al., 2018). At the same time, overly low BDOC (2-8 %) values, regardless of depth and season in humic lake and across the hydrological continuum of the bog (**Fig. 2 A**), are supportive of previous results for permafrost peatlands from the neighboring region (Shirokova et al., 2019). A general path for DOM spectral properties modification over the course of biodegradation consisted of an increase in aromaticity of DOM due to preferential uptake of non-humic low molecular weight (LMW) compounds. However, this was not accompanied by a sizable increase in SUVA (**Fig. S2**). Presumably, the proportion of these compounds in the overall DOC level was quite low and could not impact SUVA evolution. Globally, the evolution of optical ratios was consistent with bacterial consumption of aliphatic LMW compounds and an increase in the overall aromaticity of DOM.

Concerning the seasonal variation of photodegradation in the deep humic lake, maximal effects were observed in June. These effects likely occurred due to fresh terrestrial organic matter that was leached from the watershed and then efficiently processed during Arctic summer. It should be noted that labile phenolic, carbohydrates, N-containing bases and smaller molecular weight compounds are abundant in litter leachates produced during initial decay stages (Kiikkilä et al., 2011, 2012, 2013; Hensgens et al., 2021). By July, most of the biodegradable DOM was already removed, and in October, the effects were much lower. Therefore, photolabile DOM is

delivered from the forested watershed to the lake essentially during surface flux, at high water flow. It is then quickly removed from the water column, which was especially seen in the 0.5 and 5 m horizons of Lake Temnoe. Although labile organic matter from litter fall was also delivered during autumn rain season, presumably, during this period, the conditions for photolysis (low temperature, short daytime period and insufficient light) were not as favorable as those in June or August.

Photodegradation of waters from the Ilasskoe Bog continuum demonstrated maximal rates in the piezometer (**Fig. 3 B**). During photolysis of humic water, a decrease in optical ratios (E_{365}:E_{470}; E_{470}:E_{665}) clearly indicated preferential degradation of humic aromatic compounds. The strong effect of photodegradation on DOM optical properties in the 650-500 nm region may be linked to decomposition of complex DOM into smaller molecules, whereas a decrease of absorbance in the 230-400 nm region (**Fig. S12**) indicates degradation of aromatic compounds, progressively increasing over insolation time. A recent study of DOM photolysis in humic-rich forested streams demonstrated that high aromatic material was photochemically converted into smaller non-fluorescent molecules (Wilske et al., 2020).

Results obtained on the more important role of photodegradation over biodegradation are generally consistent with earlier reports on the dominance of photolysis for DOM processing in Arctic waters within North America (Cory et al., 2014; Ward et al., 2017), the Canadian temperate zone (Winter et al., 2007; Porcal et al., 2013, 2014, 2015), and Swedish headwater catchments (Köhler et al., 2002). According to former results for Scandinavian surface waters, the main impact of DOM photolysis is reflected by a decrease in the proportion of aromatic (colored) DOC and a rather small (≤ 10 %) change in bulk DOC concentration (Groeneveld et al., 2016; Koehler et al., 2014), Canada (Laurion and Mladenov, 2013; Gareis and Lesack, 2018) and NW Russia (Oleinikova et al., 2017; Chupakova et al., 2018).

554   As a further perspective of this work, one has to consider biodegradation of photolytically

555   altered DOM given that photo-oxidation is known to transform molecular structures into more

556   bioavailable forms (e.g., Cory and Kling, 2018; Sulzberger et al., 2019) thereby stimulating

557   microbial growth under sunlight, as is known for other Arctic and subarctic settings (i.e.,

558   Drozodova et al., 2020; Laurion et al., 2020).

559

560   *4.2. Possible impact of microbial and photolytic processing on CO_2 emissions from*

561   *water surfaces*

562   A broad importance of DOM bio- and photodegradation dynamics is that these processes

563   can contribute to CO_2 emissions from water surfaces thereby directly controlling the C cycling

564   between the land and the atmopshere (Lapierre et al., 2013; Tranvik et al., 2009; Cory et al.,

565   2014, 2018). In this study, we attempted to relate, for the first time for several diverse aquatic

566   systems across seasons, experimentally measured rates of DOM degradation to in-situ measured

567   CO_2 emissions. The integral rates of DOM bioprocessing in the water column of Lake Temnoe

568   (**Table 3, Fig. 4 A**) allow quantifying the potential contribution of biodegradation to CO_2

569   production and emission. Assuming all biodegraded DOM is transformed into CO_2 and there is

570   no biomass increase or sedimentation, a 1 m water layer of the lake can emit 1.7 mmol CO_2 m^{-2}

571   d^{-1} in June and 3.3 mmol CO_2 m^{-2} d^{-1} in October. Therefore, integral flux from 10 m deep water

572   layer amounts to 17 – 33 mmol CO_2 m^{-2} d^{-1} across the seasons. These values are comparable to

573   typical values of CO_2 evasion from the surface of this lake during different seasons (30-70 mmol

574   CO_2 m^{-2} d^{-1}; **Table 1 B**). For surface waters of Ilasskoe Bog, maximal CO_2 production due to

575   DOM biomineralization alone (**Table 3**) ranged from 5.0 mmol CO_2 m^{-2} d^{-1} for the peatland pool

576   (2 m deep) to 2.5 mmol CO_2 m^{-2} d^{-1} for the outlet stream (0.5 m deep). However, in summer, the

577   peatland pool and stream emitted 23 and 150 mmol CO_2 m^{-2} d^{-1} (**Table 1 A**) which could not be

578   sustained by DOM biodegradation.

579   The addition of photodegradation (assuming a photic layer depth of 3.5 m) to DOM

580   bioprocessing in the water column of the Temnoe Lake during open water season can further

581   increase potential CO_2 production in the water column. For the case of Ilasskoe Bog waters, the

582   addition of photolytic degradation increases projected CO_2 emission from the outlet stream by a

583   factor of 5, which is still below the actual CO_2 flux, whereas DOM photolysis has no impact on

584   CO_2 emissions from the peatland pool. Note that, although the depth of sunlight processing in

585   boreal waters is typically 1-0.8 m (Vähätalo et al., 2000; Koehler et al., 2014), a more recent

586   study concluded that direct photomineralization of DOM in Artic humic ponds is limited to the

587   first centimeters of the water column (Mazoyer et al., 2022). Furthermore, in typical DOM-rich

588   Arctic waters, only half of sunlight-associated DOC losses is converted into CO_2 and the rest

589   may be turned into particles through photoflocculation (e.g., Mazoyer et al., 2022). Therefore,

590   despite a faster photodegradation rate compared to biodegradation, due to the shallow photic

591   layer in humic waters, the biodegradation may provide the largest impact on CO_2 emission from

592   the water column of boreal waters.

593   At the same time, our assumption that all CO_2 in lake water is produced by bio- or

594   photodegradation of DOM might not be warranted because there are multiple sources of CO_2 in

595   the lake waters, which were not assessed in the present study. These including but not limited to:

596   particulate organic matter bio- and photodegradation, whose importance can strongly exceed that

597   of DOC (e.g., Attermeyer et al., 2018; Keskitalo et al., 2022), sediment respiration, plankton and

598   periphyton diel photosynthetic cycle, underground water discharge at the lake bottom, and

599   delivery of DOC and CO_2-rich waters via lateral surface and shallow subsurface influx. Given

600   that the contribution of each CO_2 source can vary among different water bodies and across

601   seasons, the assessment of DOM bio- and photodegradation contribution to overall CO_2 flux in

602   this study should be considered as highly conservative.

603

4.3. Impact of DOM bio- and photo transformation on trace element pattern

In this study we hypothesized the following link between DOC and TE: in humic surface waters of peatlands, most TE, which include divalent transition metals (Cu, Ni, Co, Zn, Mn), toxicants (Be, Cr, Cd, Pb), trivalent and tetravalent hydrolysates (Al, Ga, Y, REE, Ti, Zr, Hf, Th), with an exception of some alkalis and oxyanions, are strongly (> 80%) associated to DOM in the form of organic, organo-ferric and organo-aluminium colloids (Pokrovsky et al., 2012, 2016). As a result, any DOM transformation processes, be it bio- or photo-degradation, may directly affect the concentration pattern of TE. Specifically, the DOM removal via photo- or bio-degradation should change the speciation of those elements, that are strongly bound to DOM such as divalent transition metals, or incorporated into organo-mineral (Fe, Al) colloids, such as trivalent and tetravalent hydrolysates (TE^{3+}, TE^{4+}). The former might either remain in solution (during photodegradation), hence not modifying their total dissolved concentration, or being taken up by growing bacteria during bio-degradation. The latter (TE^{3+}, TE^{4+}) are capable of co-precipitating with Fe and Al hydroxides, especially during photodegradation (i.e., Kopacek et al., 2005, 2006), hence being sizably removed from the aqueous solution. From the other hand, some TE are known to be photosensitive (Mn, Fe), toxic (Al, Cu, As, Cd, Pb), or potentially limiting micronutrients (Zn, Co, Ni, Mo) for the bacteria and therefore they are capable affecting the overall rate of photo- or bio-degradation.

However, contrary to our expectations, among all major and trace elements measured in the experiments, only trivalent and tetravalent hydrolysates (TE^{3+}, TE^{4+}) were impacted by both photo- and biodegradation. It is known that these elements are essentially present in the form of large molecular size, highly polymerized and presumbaly aromatic, organo-Fe/Al colloids in humic boreal/subacrtic lakes (Pokrovsky et al., 2012, 2016), rivers (Krickov et al., 2019; Pokrovsky et al., 2010), and soil porewaters (Pokrovsky et al., 2005; Raudina et al., 2021). Therefore, insoluble TE^{3+} and TE^{4+} generally followed the removal of Fe(III) in the form of

particulate Fe hydroxides, after breaking the Fe-DOM bonds that stabilized colloidal Fe(III) hydroxides. This destabilization and Fe hydroxide particle formation is known to occur either via biodegradation (i.e., Oleinikova et al., 2018) or photolysis (Kopacek et al., 2005, 2006; Oleinikova et al., 2017; Chupakova et al., 2018). At the same time, some micronutrients (V, Mn, Co, Cu and Ba) were affected solely by biodegradation. This can reflect uptake of these metals by growing bacterial cells, as is known from laboratory experiments with pure cultures of heterotrophic bacteria (Shirokova et al., 2017a).

Note that the effects of bio- and photodegradation were more pronounced for light REE (LREE) compared to heavy REE (HREE). This result is consistent with the fact that LREE have stronger association with Fe hydroxide compared to organic complexes, as known from general chemical considerations and laboratory experiments (i.e., Bau, 1999) and evidenced in various boreal and subacrtic settings (Pokrovsky et al., 2016; Krickov et al., 2019). Given that the main effect of both photolysis and biodegradation of DOM in humic Fe(III)-rich surface waters is coagulation of dissolved Fe(III) in the form of Fe oxy(hydr)oxides, the LREE are removed from solution. This removal occurs in the form of adsorbed complexes or coprecipitated with Fe oxy(hydr)oxides, while HREE remain in the form of strong aqueous complexes.

In former studies of photo- and biodegradation of surface waters from permafrost peatlands, only a few nutrients (P, Fe, Zn and V) and insoluble low mobility trace metals (Ti, Zr, Nb and Th) demonstrated a decrease in concentration (Shirokova et al., 2019). This list of elements is generally consistent with that established in the present study of humic subarctic lakes of the non-permafrost zone, except P and Zn which did not exhibit sizable removal in our experiments. It is possible that a high proportion of low molecular weight $LMW_{< 1 \text{ kDa}}$ (and thus, potentially bioavailable) forms of macro- and micronutrients, such as P and Zn, in the permafrost ice (i.e., Kuzmina et al., 2023) can be delivered to the lake and river via suprapermafrost flow (Raudina et al., 2018, 2021). This led to elevated bioavailability of these elements in permafrost

654 surface waters reported in previous works, as compared to permafrost-free boreal settings of this

655 study.

656

Conclusions

658 Seasonally resolved bio- and photo-degradability of DOM in a deep stratified lake and

659 summer measurements from a peat bog's hydrological continuum within the boreal zone

660 demonstrated that the subsurface and deep horizons of these stratified waters are mostly sensitive

661 to sunlight impact, and that maximal effects of photodegradation occurred in June, during strong

662 insolation. In contrast, the biodegradation of DOM from the humic lake was mostly pronounced

663 during October, when fresh leachates of forest litter were exported from the watershed. Insoluble,

664 low-mobility trace metals such as trivalent and tetravalent hydrolysates were affected by both

665 bio- and photodegradation, as they are associated with coagulating $Fe(III)$ oxyhydroxides.

666 A broad implication of obtained results is that, although DOM photodegradation rates

667 were sizably higher compared to those of biodegradation, the rather thin photic layer in humic

668 waters does not allow for significant contribution of photolysis in overall CO_2 emission from

669 lake and bog surfaces. Further work is needed on biodegradation of photolytically altered DOM

670 given that photo-oxidation is known to transform molecular structures into more bioavailable

671 forms. The high seasonal dynamics and spatial variability in both photo- and biodegradability of

672 DOM and related trace elements of humic surface waters in the boreal zone encountered in this

673 study suggest the need for studying these processes during "shoulder seasons" (early spring and

674 late autumn), the periods of maximal photo- and biodegradation, respectively. These efforts

675 should be focused on the most dynamic components such as small streams and subsurface waters,

676 which demonstrated the highest rates of both photo- and biodegradation.

677

678

Acknowledgements

This work was supported by RSF grant No 22-17-00253. LS and OP were also supported by project PEACE of PEPR FairCarboN ANR-22-PEXF-0011. OP is grateful for partial support from the TSU Development Programme Priority-2030.

Assets: All the data obtained in this work are presented in Supplementary Information file.

Authors contribution.

AVC and OP designed the study and wrote the paper; AC, NN and SB performed sampling, analysis and their interpretation; LS performed bacterial number assessment and DOC results interpretation; AVC, TV and OP provided analyses of literature data.

Competing interests.

The authors declare that they have no conflict of interest.

References

Abbott, B. W., Larouche, J. R., Jones, J. B., Bowden, W. B., and Balser, A. W.: Elevated dissolved organic carbon biodegradability from thawing and collapsing permafrost, J. Geophys. Res., 119, 2049–2063, https://doi.org/10.1002/2014JG002678, 2014.

Amado, A. M., Cotner, J. B., Cory, R. M., Edhlund, B. L., and McNeill, K.: Disentangling the interactions between photochemical and bacterial degradation of dissolved organic matter: amino acids play a central role, Microb. Ecol., 69(3), 554-566, doi: 10.1007/s00248-014-0512-4, 2014.

Amaral, V., Ortega, T., Romera-Castillo, C., and Forja, J.: Linkages between greenhouse gases (CO_2, CH_4, and N_2O) and dissolved organic matter composition in a shallow estuary, Sci. Total Environ. 788, Art No 147863, https://doi.org/10.1016/j.scitotenv.2021.147863, 2021.

Andersson, M. G. I., Catalán, N., Rahman, Z., Tranvik, L. J., and Lindström, E. S.: Effects of sterilization on dissolved organic carbon (DOC) composition and bacterial utilization of DOC from lakes, Aquat. Microb. Ecol., 82, 199-208, http://dx.doi.org/10.3354/ame01890, 2018.

Ask, J., Karlsson, J., and Jansson, M.: Net ecosystem production in clear-water and brown-water lakes, Glob. Biogeochem. Cycles, 26, GB1017, doi:10.1029/2010GB003951, 2012.

Attermeyer, K., Catalán, N., Einarsdottir, K., Freixa, A., Groeneveld, M., Hawkes, J. A., et al.: Organic carbon processing during transport through boreal inland waters: Particles as important sites, J. Geophys. Res.: Biogeosciences, 123(8), 2412–2428. https://doi.org/10.1029/2018jg004500, 2018.

Bau, M.: Scavenging of dissolved yttrium and rare earths by precipitating iron oxyhydroxide: experimental evidence for Ce oxidation, Y-Ho fractionation, and lanthanide tetrad effect, Geochim. Cosmochim. Ac., 63, 67–77, doi: 10.1016/S0016-7037(99)00014-9, 1999.

Battin T.J. Dissolved organic materials and its optical properties in a blackwater tributary of the upper Orinoco River, Venezuela, Organic Geochemistry, 28, 561-569, https://doi.org/10.1016/S0146-6380(98)00028-X, 1998.

Begum, M. S., Park, J.-H., Yang, L., Shin, K. H., and Hur, J.: Optiacl and molecular indices of dissolved organic matter for estimating biodegradability and resulting carbon dioxide production in inland waters: A review. Water Research, Art No 119362, https://doi.org/10.1016/j.watres.2022.119362, 2022.

Berggren, M., Laudon, H., and Jansson, M.: Landscape regulation of bacterial growth efficiency in boreal freshwaters, Global Biogeochem. Cy., 21, GB4002. http://dx.doi.org/10.1029/2006GB002844, 2007.

Berggren, M., Laudon, H., Haei, M., Ström, L., and Jansson, M.: Efficient aquatic bacterial metabolism of dissolved low-molecular-weight compounds from terrestrial sources, ISME J., 4, 408-416, https://doi.org/10.1038/ismej.2009.120, 2010.

Borges, A., Darchambeau, F., Teodoru, C. et al. : Globally significant greenhouse-gas emissions from African inland waters, Nature Geosci., 8, 637–642. https://doi.org/10.1038/ngeo2486, 2015.

Chaudhary, N., Westermann, S., Lamba, S., et al.: Modelling past and future peatland carbon dynamics across the pan- Arctic, Glob. Change Biol., 26, 4119-4133, doi: 10.1111/gcb.15099, 2020.

Chin, Y.-P., Aiken, G., and O'Loughlin, E.: Molecular weight, polydispersity, and spectroscopic properties of aquatic humic substances, Environ. Sci. Technol., 28, 1853-1858, https://pubs.acs.org/doi/10.1021/es00060a015, 1994.

Chupakov, A., Ershova, A., Moreva, O. Yu, Shirokova, L. S., Zabelina, S. A., Vorobieva, T.Ya., Klimov, S. I., Brovkon N., Pokrovsky, O.S.: Seasonal dynamics of dissolved carbon in contrasting stratified lakes of the subarctic, Boreal Environ. Res., 22, 213–230, https://www.borenv.net/BER/archive/pdfs/ber22/ber22-213-230.pdf, 2017.

Chupakova, A. A., Chupakov, A. V., Neverova, N. V., Shirokova, L. S., and Pokrovsky, O. S.: Photodegradation of river dissolved organic matter and trace metals in the largest European Arctic estuary, Sci. Total Environ., 622–623, 1343–1352, http://dx.doi.org/10.1016/j.scitotenv.2017.12.030, 2018.

Cole, J. J. and Caraco, N.: Atmospheric exchange of carbon dioxide in a low-wind oligotrophic lake measured by the addition of SF6, Limnol. Oceanog., 43, 647–656, https://doi.org/10.4319/lo.1998.43.4.0647, 1998.

Cole, J. J., Prairie, Y. T., Caraco, N. F., McDowell, W. H., Tranvik, L. J., Striegl, R. G., Duarte, C. M., Kortelainen, P., Downing, J. A., Middelburg, J. J., and Melack, J.: Plumbing the global carbon cycle: Integrating inland waters into the terrestrial carbon budget, Ecosystems, 10, 172–185, https://doi.org/10.1007/s10021-006-9013-8, 2007.

Cory, R. M., Ward, C. P., Crump, B. C., and Kling, G. W.: Sunlight controls water column processing of carbon in arctic fresh waters, Science, 345, 925-928, https://doi.org/10.1126/science.1253119, 2014.

Cory, R. M., and Kling, G. W.: Interactions between sunlight and microorganisms influence dissolved organic matter degradation along the aquatic continuum, Limnol. Oceanogr. Lett., 3, 102–116, https://doi.org/10.1002/lol2.10060, 2018.

Dean, J. F., van Hal, J. R., Dolman, A. J., Aerts, R., and Weedon, J. T.: Filtration artefacts in bacterial community composition can affect the outcome of dissolved organic matter biolability assays, Biogeosciences, 15, 7141-7154, https://doi.org/10.5194/bg-15-7141-2018, 2018.

Dean, J. F., Garnett, M. H., Spyrakos, E., Billett, M. F.: The potential hidden age of dissolved organic carbon exported by peatland streams, J. Geophys. Res.: Biogeosciences, 124, 328–341, http://dx.doi.org/10.1029/2018JG004650, 2019.

Don, A., and Kalbitz, K.: Amount and degradability of dissolve dorganic carbon from foliar litter at different decomposition stages, Soil Biol. Biochem., 37, 2171-2179, http://dx.doi.org/10.1016/j.soilbio.2005.03.019, 2005.

Drozdova, O. Y., Aleshina, A. R., Tikhonov, V. V., Lapitskiy, S. A., and Pokrovsky, O. S.: Coagulation of organo-mineral colloids and formation of bioavailable low molecular weight organic complexes in boreal humic river water under UV-irradiation, Chemosphere, 250, Art No 126216, doi.org/10.1016/j.chemosphere.2020.126216, 2020.

Gareis, J. A. L., and Lesack, L. F. W.: Photodegraded dissolved organic matter from peak freshet river discharge as a substrate for bacterial production in a lake-rich great Arctic delta, Arctic Science, 4(4), 557-583, http://dx.doi.org/10.1139/AS-2017-0055, 2018.

Groeneveld, M., Tranvik, L., Natchimuthu, S., and Koehler, B.: Photochemical mineralisation in a boreal brown water lake: considerable temporal variability and minor contribution to carbon dioxide production, Biogeoscience, 13, 3931-3943, https://doi.org/10.5194/bg-13-3931-2016, 2016.

Harris, L. I., Richardson, K., Bona, K. A., Davidson, S. J., Finkelstein, S. A., Garneau, M., McLaughlin, J., Nwaishi, F., Olefeldt, D., Packalen, M., Roulet, N. T., Southee, F. M., Strack, M., Webster, K. L., Wilkinson, S. L., and Ray, J. C.: The essential carbon service provided by northern peatlands, Front. Ecol. Environ., 20, 222–230, https://doi.org/10.1002/fee.2437, 2022.

Hengsgens, G., Lechtenfeld, O. J., Guillemette, F., Laudon, H., Berggren, M.: Impacts of litter decay on organic leachate composition and reactivity, Biogeochemistry 154, 99-117, https://link.springer.com/article/10.1007/s10533-021-00799-3, 2021.

Hiriart-Baer, V.P., Diep, N., and Smith, R.E.H.: Dissolved organic matter in the Great Lakes: role and nature of allochthonous material, J. Great Lakes Res. 34, 383–394, https://doi.org/10.3394/0380-1330(2008)34[383:DOMITG]2.0.CO;2, 2008.

Hur, J., Williams, M. A., and Schlautman, M. A.: Evaluating spectroscopic and chromatographic techniques to resolve dissolved organic matter via end member mixing analysis, Chemosphere, 63, 387-402, https://doi.org/10.1016/j.chemosphere.2005.08.069, 2006.

Ilina, S. M., Drozdova, O. Yu., Lapitsky, S. A., Alekhin, Yu. V., Demin, V. V., Zavgorodnaya, Yu. A., Shirokova, L. S., Viers, J., and Pokrovsky, O. S.: Size fractionation and optical properties of dissolved organic matter in the continuum soil solution-bog-river and terminal lake of a boreal watershed, Org. Geochem., 66, 14–24, http://dx.doi.org/10.1016/j.orggeochem.2013.10.008, 2014.

Kalbitz, K., Schmerwitz, J., Schwesig, D., and Matzner, E.: Biodegradation of soil-derived dissolved organic matter as related to its properties, Geoderma 113, 273-291, https://doi.org/10.1016/S0016-7061(02)00365-8, 2003.

Karlsson, J., Serikova, S., Rocher-Ros, G., Denfeld, B., Vorobyev, S. N., Pokrovsky, O. S.: Carbon emission from Western Siberian inland waters, Nature Comm., 12, 825, https://doi.org/10.1038/s41467-021-21054-1, 2021.

Kawahigashi, M., Kaiser, L., Kalbitz, K., Rodionov, A., and Guggenberger, G.: Dissolved organic matter in small streams along a gradient from discontinuous to continuous permafrost. Global Change Biol. 10, 1576-1586, https://doi.org/10.1111/j.1365-2486.2004.00827.x, 2004.

Keskitalo, K.H., Bröder, L., Jong, D., Zimov, N., Davydova, A., Davydov, S., Tesi, T., Mann, P. J., Haghipour, N., Eglinton, T. I., and Vonk, J. E.: Seasonal variability in particulate organic

carbon degradation in the Kolyma River, Siberia. Environmental Research Letters, 17(3), Art No 034007. DOI 10.1088/1748-9326/ac4f8d, 2022.

Kiikkkilä, O., Kitunen, V., and Smolander, A.: Properties of dissolved organic matter derived from silver birch and Norway spruce stands: Degradability combined with chemical characteristics, Soil Biol. Biochem. 43, 421-430, http://dx.doi.org/10.1016/j.soilbio.2010.11.011, 2011.

Kiikkkilä, O., Kitunen, V., Spetz, P., and Smolander, A.: Characterization of dissolved organic matter in decomposing Norway spruce and silver birch litter, European J Soil Sci 63, 476-486, http://dx.doi.org/10.1111/j.1365-2389.2012.01457.x, 2012.

Kiikkkilä, O., Smolander, A., and Kitunen, V.: Degradability, molecular weight and adsorption properties of dissolved organic carbon and nitrogen leached from different types of decomposing litter, Plant Soil 373, 787-798, https://doi.org/10.1016/j.femsec.2004.08.011, 2013.

Koehler, B., Landelius, T., Weyhenmeyer, G. A., Machida, N., and Tranvik, L.J.: Sunlight-induced carbon dioxide emissions from inland waters, Global Biogeochem. Cycles, 28, 696–711, https://doi.org/10.1002/2014GB004850, 2014.

Köhler, S., Buffam, I., Jonsson, A., and Bishop, K.: Photochemical and microbial processing of stream and soil water dissolved organic matter in a boreal forested catchment in northern Sweden, Aquat. Sci., 64, 269–281, http://dx.doi.org/10.1007/s00027-002-8071-z, 2002.

Kopáček, J., Klementova, S., and Norton S. A.: Photochemical production of ionic and particulate aluminum and iron in lakes, Environ. Sci. Technol., 39, 3656–3662, https://pubs.acs.org/doi/10.1021/es048101a, 2005.

Kopáček, J., Marešová, M., Norton, S. A., Porcal, P., and Veselý, J.: Photochemical source of metals for sediments, Environ. Sci. Technol., 40(14), 4455–4459. https://doi.org/10.1021/es0600532, 2006.

Krickov, I. V., Pokrovsky, O. S., Manasypov, R. M., Lim, A., Shirokova, L. S., and Loiko, S. V.: Colloidal transport of carbon and metals by western Siberian rivers during different seasons across a permafrost gradient, Geochim. Cosmochim. Acta 265, 221-241, https://doi.org/10.1016/j.gca.2019.08.041, 2019.

Kuzmina, D., Lim, A. G., Loiko, S. V, Shirokova, L. S., Julien, F., Rols, J. L., and Pokrovsky, O. S.: Dispersed ice of permafrost peatlands represents an important source of labile carboxylic acids, nutrients and metals, Geoderma, 429, Art No 116256. https://doi.org/10.1016/j.geoderma.2022.116256, 2023.

Lapierre, J.-F., Guillemette, F., Berggren, M., and del Giorgio, P. A.: Increases in terrestrially derived carbon stimulate organic carbon processing and CO_2 emissions in boreal aquatic ecosystems, Nature Comm., 4, 2972, doi:10.1038/ncomms3972, 2013.

Larouche, J. R., Abbott, B. W., Bowden, W. B., Jones, and J. B.: The role of watershed characteristics, permafrost thaw, and wildfire on dissolved organic carbon biodegradability and water chemistry in Arctic headwater streams, Biogeosciences, 12, 4221-4233, https://doi.org/10.5194/bg-12-4221-2015, 2015.

Lau, M. P.: Linking the dissolved and particulate domain of organic carbon in inland waters. J. Geophys. Res.: Biogeosciences, 126, e2021JG006266. https://doi.org/10.1029/2021JG006266, 2021.

Laurion, I., and Mladenov, N.: Dissolved organic matter photolysis in Canadian Arctic thaw ponds, Environ. Res. Lett., 8, 035026, doi.org/10.1088/1748-9326/8/3/035026, 2013.

Laurion, I., Massicotte, P., Mazoyer, F., Negandhi, K., and Mladenov, N.: Weak mineralization despite strong processing of dissolved organic matter in Eastern Arctic tundra ponds, Limnol. Oceanogr., 66, S47–S63, https://doi.org/10.1002/lno.11634, 2021.

Liu, F., and Wang, D.: Dissolved organic carbon concentration and biodegradability across the global rivers: A meta-analysis, Sci. Total Environ., 818, Art No 151828, https://doi.org/10.1016/j.scitotenv.2021.151828, 2022.

Lou, T., and Xie, H.: Photochemical alteration of the molecular weight of dissolved organic matter, Chemosphere, 65, 2333-2342, https://doi.org/10.1016/j.chemosphere.2006.05.001, 2006.

Mann, P. J., Davydova, A., Zimov, N., Spencer, R. G. M., Davydov, S., Bulygina, E., Zimov, S., Holmes, R. M.: Controls on the composition and lability of dissolved organic matter in Siberia's Kolyma River basin, J. Geophys. Res., 117, G01028, doi: 10.1029/2011JG001798, 2012.

Mann, P. J., Sobczak, W. V., LaRue, M. M., Bulygina, E., Davydova, A., Vonk, J. E., Schade, J., Davydov, S., Zimov, N., Holmes, R. M., Spencer, R. G. M.: Evidence for key enzymatic controls on metabolism of Arctic river organic matter, Global Change Biol., 20(4), 1089-1100, https://doi.org/10.1111/gcb.12416, 2014.

Mann, P. J., Eglinton, T. I., Mcintyre, C. P., Zimov, N., Davydova, A., Vonk, J. E., Holmes, R. M., Spencer, R. G. M.: Utilization of ancient permafrost carbon in headwaters of Arctic fluvial networks, Nat. Commun., 6, doi: 10.1038/ncomms8856, 2015.

Mazoyer, F., Laurion, I., and Rautio, M.: The dominant role of sunlight in degrading winter dissolved organic matter from a thermokarst lake in a subarctic peatland, Biogeosciences, 19, 3959–3977, https://doi.org/10.5194/bg-19-3959-2022, 2022.

Moody, C. S., Worrall, F., Evans, C. D., Jones, T. G.: The rate of loss of dissolved organic carbon (DOC) through a catchment, J. Hydrol., 492, 139-150, https://doi.org/10.1016/j.jhydrol.2013.03.016, 2013.

Moran, M. A., Sheldon, W. M., and Zepp, R. G.: Carbon loss and optical property changes during long-term photochemical and biological degradation of estuarine dissolved organic matter, Limnol. Oceanogr., 45, 1254–1264, https://doi.org/10.4319/lo.2000.45.6.1254, 2000.

Mostofa, K. M. G., Yoshioka, T., Konohira, E., and Tanoue, E.: Photodegradation of fluorescent dissolved organic matter in river waters, Geochem. J., 41, 323-331, https://doi.org/10.2343/geochemj.41.323, 2007.

Obernosterer, I., and Benner, R.: Competition between biological and photochemical processes in the mineralization of dissolved organic carbon, Limnol. Oceanogr., 49, 117–124, https://doi.org/10.4319/lo.2004.49.1.0117, 2004.

Oleinikova, O., Drozdova, O. Y., Lapitskiy, S. A., Bychkov, A. Y., and Pokrovsky, O. S.: Dissolved organic matter degradation by sunlight coagulates organo-mineral colloids and produces low-molecular weight fraction of metals in boreal humic waters, Geochim. Cosmochim. Acta, 211, 97-114, doi:10.1016/j.gca.2017.05.023, 2017.

Oleinikova, O., Shirokova, L. S., Drozdova, O. Y., Lapitsky, S. A., and Pokrovsky, O. S.: Low biodegradability of dissolved organic matter and trace metal from subarctic waters by culturable heterotrophic bacteria, Sci. Total Environ., 618, 174-187, https://doi.org/10.1016/j.scitotenv.2017.10.340, 2018.

Payandi-Rolland, D.; Shirokova, L.S.; Tesfa, M.; Lim, A.G.; Kuzmina, D.; Benezeth, P.; Karlsson, J.; Giesler, R.; Pokrovsky, O.S.: Dissolved organic matter biodegradation along a hydrological continuum in a discontinuous permafrost area: Case study of northern Siberia and Sweden, Sci. Total Environ., 749, Art No 141463, https://doi.org/10.1016/j.scitotenv.2020.141463, 2020.

Peacock, M., Evans, C. D., Fenner, N., Freeman, C., Gough, R., Jones, T. G., and Lebron, I.: UV-visible absorbance spectroscopy as a proxy for peatland dissolved organic carbon (DOC) quantity and quality: considerations on wavelength and absorbance degradation, Environmental Science: Processes and Impacts, 10–12, doi:10.1039/c4em00108g, 2014.

Pickard, A. E., Heal, K. V., McLeod, A. R., and Dinsmore, K. J.: Temporal changes in photoreactivity of dissolved organic carbon and implications for aquatic carbon fluxes from peatlands, Biogeosciences, 14, 1793-1809, https://doi.org/10.5194/bg-14-1793-2017, 2017.

Pokrovsky, O. S., Dupré, B., and Schott, J.: Fe-Al-organic colloids control the speciation of trace elements in peat soil solutions: results of ultrafiltration and dialysis, Aquatic Geochem., 11, 241-278, http://dx.doi.org/10.1007/s10498-004-4765-2, 2005.

Pokrovsky, O. S., Viers, J., Shirokova, L. S., Shevchenko, V. P., Filipov, A. S., and Dupré, B.: Dissolved, suspended, and colloidal fluxes of organic carbon, major and trace elements in Severnaya Dvina River and its tributary, Chem. Geol., 273, 136–149, https://doi.org/10.1016/j.chemgeo.2010.02.018, 2010.

Pokrovsky, O. S., Shirokova, L. S., Zabelina, S. A., Vorobieva, T. Ya., Moreva, O. Yu., Klimov, S. I, Chupakov, A. V., Shorina, N. V., Kokryatskaya, N. M., Audry, S., Viers, J., Zoutien, C., and Freydier, R.: Size fractionation of trace elements in a seasonally stratified boreal lakes: Control of organic matter and iron colloids, Aquat. Geochem., 18, 115–139, https://doi.org/10.5194/bg-16-2511-2019, 2012.

Pokrovsky, O. S., Manasypov, R. M., Loiko, S. V., and Shirokova, L. S.: Organic and organo-mineral colloids of discontinuous permafrost zone, Geochim. Cosmochim. Ac., 188, 1–20, http://dx.doi.org/10.1016/j.gca.2016.05.035, 2016.

Porcal, P., Dillon, P. J., and Molot, L. A.: Photochemical production and decomposition of particulate organic carbon in a freshwater stream, Aquat. Sci., 75, 469–482, http://dx.doi.org/10.1007/s00027-013-0293-8, 2013.

Porcal, P., Dillon, P. J., and Molot, L. A.: Interaction of extrinsic chemical factors affecting photodegradation of dissolved organic matter in aquatic ecosystems, Photochem. Photobiol. Sci., 13, 799-812, http://dx.doi.org/10.1039/c4pp00011k, 2014.

Porcal, P., Dillon, P. J., and Molot, L. A.: Temperature dependence of photodegradation of dissolved organic matter to dissolved inorganic carbon and particulate organic carbon, Plos ONE, 10(6), e0128884, doi:10.1371/journal.pone.0128884, 2015.

Prijac, A., Gandois, L., Jeanneau, L., Taillardat, P., and Garneau, M.: Dissolved organic matter concentration and composition discontinuity at the peat–pool interface in a boreal peatland, Biogeosciences, 19, 4571–4588, https://doi.org/10.5194/bg-19-4571-2022, 2022.

Raudina, T. V., Loiko, S. V., Lim, A., Manasypov, R. M., Shirokova, L. S., Istigecgev, G. I., Kuzmina, D. M., Kulizhsky, S. P., Vorobyev, S. N., and Pokrovsky, O. S.: Permafrost thaw and climate warming may decrease the CO_2, carbon, and metal concentration in peat soil waters of the Western Siberia Lowland, Sci. Total Environ., 634, 1004-1023, http://dx.doi.org/10.1016/j.scitotenv.2018.04.059, 2018.

Raudina, T. V., Loiko, S., Kuzmina, D. M., Shirokova, L. S., Kulizhsky, S. P., Golovatskaya, E. A., and Pokrovsky, O. S.: Colloidal organic carbon and trace elements in peat porewaters across a permafrost gradient in Western Siberia, Geoderma 390, Art No 114971, https://doi.org/10.1016/j.geoderma.2021.114971, 2021.

Raudina, T. V., Smirnov, S. V., Luschaeva, I. V., Kulizhskiy, S. P., Golovatskaya, E. A., Shirokova, L.S., and Pokrovsky, O. S.: Seasonal and spatial variations of dissolved organic

matter biodegradation along the aquatic continuum in the southern taiga bog complex, Western Siberia. Water (MDPI), 14, Art No 3969. https://doi.org/10.3390/w1423396, 2022.

Roehm, C. L., Giesler, R., Karlsson, J.: Bioavailability of terrestrial organic carbon to lake bacteria: The case of a degrading subarctic permafrost mire complex, J. Geophys. Res., 114, G03006, doi: 10.1029/2008JG000863, 2009.

Rosset, T., Binet, S., Rigal, F., and Gandois, L.: Peatland dissolved organic carbon export to surface waters: Global significance and effects of anthropogenic disturbance, Geophysical Res. Lett., 49, e2021GL096616. https://doi.org/10.1029/2021GL096616, 2022.

Selvam, B. P., Lapierre, J.-F., Guillemette, F., Voigt, C., Lamprecht, R. E., Biasi, C., Christensen, T. R., Martikainen P. J., and Berggren, M.: Degradation potentials of dissolved organic carbon (DOC) from thawed permafrost peat, Scientific Reports, 7, Art No 45811, doi: 10.1038/srep45811, 2016.

Serikova, S., Pokrovsky, O. S., Ala-aho, P., Kazantsev, V., Kirpotin, S. N. Kopysov, S. G., Krickov, I. V., Laudon, H., Manasypov, R. M., Shirokova, L. S., Sousby, C., Tetzlaff, D., and Karlsson, J.: High riverine CO_2 emissions at the permafrost boundary of Western Siberia. Nature Geoscience, 11, 825-829, https://www.nature.com/articles/s41561-018-0218-1, 2018.

Serikova, S., Pokrovsky, O. S., Laudon, H., Krickov, I. V., Lim, A. G., Manasypov, R. M., and Karlsson, J.: C emissions from lakes across permafrost gradient of Western Siberia, Nature Comm. 10, Art No 1552, https://doi.org/10.1038/s41467-019-09592-1, 2019.

Shirokova, L. S., Bredoire, R., Rolls, J. L., and Pokrovsky, O. S.: Moss and peat leachate degradability by heterotrophic bacteria: fate of organic carbon and trace metals, Geomicrobiol. J., 34(8), 641-655, http://dx.doi.org/10.1080/01490451.2015.1111470, 2017a.

Shirokova, L. S., Chupakova, A. A., Chupakov, A. V., and Pokrovsky, O.S.: Transformation of dissolved organic matter and related trace elements in the mouth zone of the largest European Arctic river: experimental modeling, Inland Waters, 7(3), 272-282, https://doi.org/10.6084/m9.figshare.5387686, 2017b.

Shirokova, L. S., Labouret, J., Gurge, M., Gerard, E., Zabelina, S. A., Ivanova, I. S., Pokrovsky, O. S.: Impact of cyanobacterial associate and heterotrophic bacteria on dissolved organic carbon and metal in moss and peat leachate: application to permafrost thaw in aquatic environments, Aquatic Geochemistry, 23(5–6), 331–358, https://doi.org/10.1007/s10498-017-9325-7, 2017c.

Shirokova, L. S., Chupakov, A. V., Zabelina, S. A., Neverova, N. V., Payandi-Rolland, D., Causseraund, C., Karlsson, J., and Pokrovsky, O. S.: Humic surface waters of frozen peat bogs (permafrost zone) are highly resistant to bio- and photodegradation, Biogeosciences, 16, 2511–2526, https://doi.org/10.5194/bg-16-2511-2019, 2019.

Shirokova, L. S., Chupakov, A. V., Ivanova, I. S., Moreva, O. Y., Zabelina, S. A., Shutskiy, N. A., Loiko S. V., Pokrovsky, O. S. Lichen, moss and peat control of C, nutrient and trace metal regime in lakes of permafrost peatlands. Science Total Environ., 782, Art No 146737, https://doi.org/10.1016/j.scitotenv.2021.146737, 2021.

Spencer, R. G. M., Mann, P. J., Dittmar, T., Eglinton, T. I., McIntyre, C., Holmes, R. M., Zimov, N., Stubbins, A.: Detecting the signature of permafrost thaw in Arctic rivers, Geophys. Res. Lett., 42, 2830-2835, https://doi.org/10.1002/2015GL063498, 2015.

Stubbins, A., Spencer, R.G., Chen, H., Hatcher, P.G., Mopper, K.W., Hernes, P.J., Mwamba, V., Mangangu, A.M., Wabakanghanzi, J.N., and Six, J.: Illuminated darkness: Molecular signatures of Congo River dissolved organic matter and its photochemical alteration as

revealed by ultrahigh precision mass spectrometry. Limnol. Oceanogr., 55(4), 1467-1477, 10.4319/lo.2010.55.4.1467, 2010.

Stutter, M. I., Richards, S., and Dawson, J. J. C.: Biodegradability of natural dissolved organic matter collected from a UK moorland stream, Water Res., 47(3), 1169-1180, https://doi.org/10.1016/j.watres.2012.11.035, 2013.

Sulzberger, B., Austin, A. T., Cory, R. M., Zepp, R. G., and Paul, N. D.: Solar UV radiation in a changing world: roles of cryosphere-land-water-atmosphere interfaces in global biogeochemical cycles, Photochem. Photobiol. Sci., doi: 10.1039/c8pp90063a, 2019.

Taillardat, P., Bodmer, P., Deblois, C. P., Ponçot, A., Prijac, A., Riahi, K., et al. : Carbon dioxide and methane dynamics in a peatland headwater stream: Origins, processes and implications, J. Geophysical Res.: Biogeosciences, 127, e2022JG006855. https://doi.org/10.1029/2022JG006855, 2022.

Textor, S. R., Guillemette, F., Zito, P. A., Spencer, R. G. M.: An assessment of dissolved organic carbon biodegradability and priming in blackwater systems, J. Geophys. Res. Biogeosciences, 123(9), 2998-3015, https://doi.org/10.1029/2018JG004470, 2018.

Tranvik, L. J., Downing, J. A., Cotner, J. B., Loiselle, S. A., Striegl, R. G., Ballatore, T. J., Dillon, P., Finlay, K., Fortino, K., Knoll, L. B., Kortelainen, P. L., Kutser, T., Larsen, S., Laurion, I., Leech, D. M., McCallister, S. L., McKnight, D. M., Melack, J. M., Overholt, E., Porter, J. A., Prairie, Y., Renwick, W. H., Roland, F., Sherman, B. S., Schindler, D. W., Sobek, S., Tremblay, A., Vanni, M. J., Verschoor, A. M., von Wachenfeldt, E., and Weyhenmeyer, G. A.: Lakes and reservoirs as regulators of carbon cycling and climate, Limnol. Oceanogr., 54, 2298–2314, https://doi.org/10.4319/lo.2009.54.6_part_2.2298, 2009.

Vachon, D., Lapierre, J., and del Giorgio, P. A.: Seasonality of photochemical dissolved organic carbon mineralization and its relative contribution to pelagic CO_2 production in northern lakes, J. Geophys. Res.-Biogeo., 121, 864–878, https://doi.org/10.1002/2015JG003244, 2016.

Vachon, D., Solomon, C. T., and del Giorgio, P. A.: Reconstructing the seasonal dynamics and relative contribution of the major processes sustaining CO_2 emissions in northern lakes, Limnol. Oceanogr., 62, 706–722, https://doi.org/10.1002/lno.10454, 2017.

Vähätalo, A. V., Salonen, K., Münster, U., Järvinen, M., and Wetzel, R. G.: Photochemical transformation of allochthonous organic matter provides bioavailable nutrients in a humic lake, Acta Hydrobiol., 156, 287-314, http://dx.doi.org/10.1127/0003-9136/2003/0156-0287, 2003.

Vähätalo, A. V. and Wetzel, R.G.: Photochemical and microbial decomposition of chromophoric dissolved organic matter during long (months-years) exposures, Mar. Chem., 89, 313-326, http://dx.doi.org/10.1016/j.marchem.2004.03.010, 2004.

Vasyukova, E., Pokrovsky, O. S., Viers, J., Oliva, P., Dupré, B., Martin, F., and Candaudap, F.: Trace elements in organic- and iron-rich surficial fluids of boreal zone: Assessing colloidal forms via dialysis and ultrafiltration, Geochim. Cosmochim. Acta, 74, 449-468, https://doi.org/10.1016/j.crte.2012.08.003, 2010.

Vonk, J. E., Tank, S. E., Mann, P. J., Spencer, R. G. M., Treat, C. C., Striegl, R. G., Abbott, B. W., and Wickland K. P.: Biodegradability of dissolved organic carbon in permafrost soils and aquatic systems: a meta-analysis, Biogeosciences, 12, 6915-6930, https://doi.org/10.5194/bg-12-6915-2015, 2015.

Ward, C. P., Nalven, S. G., Crump, B. C., Kling, G. W., and Cory, R. M.: Photochemical alteration of organic carbon draining permafrost soils shifts microbial metabolic pathways and stimulates respiration, Nature Comm., 8, Art No 772, https://www.nature.com/articles/s41467-017-00759-2, 2017.

1049 Wauthy, M., Rautio, M., Christoffersen, K. S., Forsstrom, L., Laurion, I., Mariash, H. L.,
1050   Peura, S., Vincent, W. F.: Increasing dominance of terrigenous organic matter in
1051   circumpolar freshwaters due to permafrost thaw, Limnol. Oceanogr. Lett., 3, 2018, 186–
1052   198, http://dx.doi.org/10.1002/lol2.10063, 2012.
1053 Weishaar, J. L., Aiken, G. R., Bergamaschi, B. A., Fram, M. S., Fujii, R., and Mopper, K.:
1054   Evaluation of specific ultraviolet absorbance as an indicator of the chemical composition
1055   and reactivity of dissolved organic carbon, Environ. Sci. Technol., 37, 4702–4708,
1056   http://dx.doi.org/10.1021/es030360x, 2003.
1057 Wickland, K. P., Aiken G. R., Butler K., Dornblaser M. M., Spencer R. G. M., and Striegl R.
1058   G.: Biodegradability of dissolved organic carbon in the Yukon River and its tributaries:
1059   seasonality and importance of inorganic nitrogen. Glob Biogeochem Cycle 26,
1060   2012gb004342, http://dx.doi.org/10.1029/2012GB004342, 2012.
1061 Wilske, C., Herzsprung, P., Lechtenfeld, O.J., Kamjunke, N., and von Tümpling, W.:
1062   Photochemically induced changes of dissolved organic matter in a humic-rich and forested
1063   stream, Water, 12, 331. https://doi.org/10.3390/w12020331, 2020.
1064 Winter, A. R., Fish, T. A. E., Playle, R. C., Smith, D. S., and Curtis, P. J.: Photodegradation of
1065   natural organic matter from diverse freshwater sources, Aquat. Toxicol., 84, 215-222,
1066   https://doi.org/10.1016/j.aquatox.2007.04.014, 2007.
1067 Zabelina, S.A., Shirokova, L.S., Klimov, S.I., Chupakov, A.V., Lim, A.G., Polishchuk, Y.M.,
1068   Polishchuk, V.Y., Bogdanov, A.N., Muratov, I.N., Guerin, F., Karlsson, J., and Pokrovsky,
1069   O.S.: Carbon emission from thermokarst lakes in NE European tundra, Limnol. Oceanogr.,
1070   66, S216-S230. https://doi.org/10.1002/lno.11560, 2021.

1071

1072

1073

1074

1075

1076
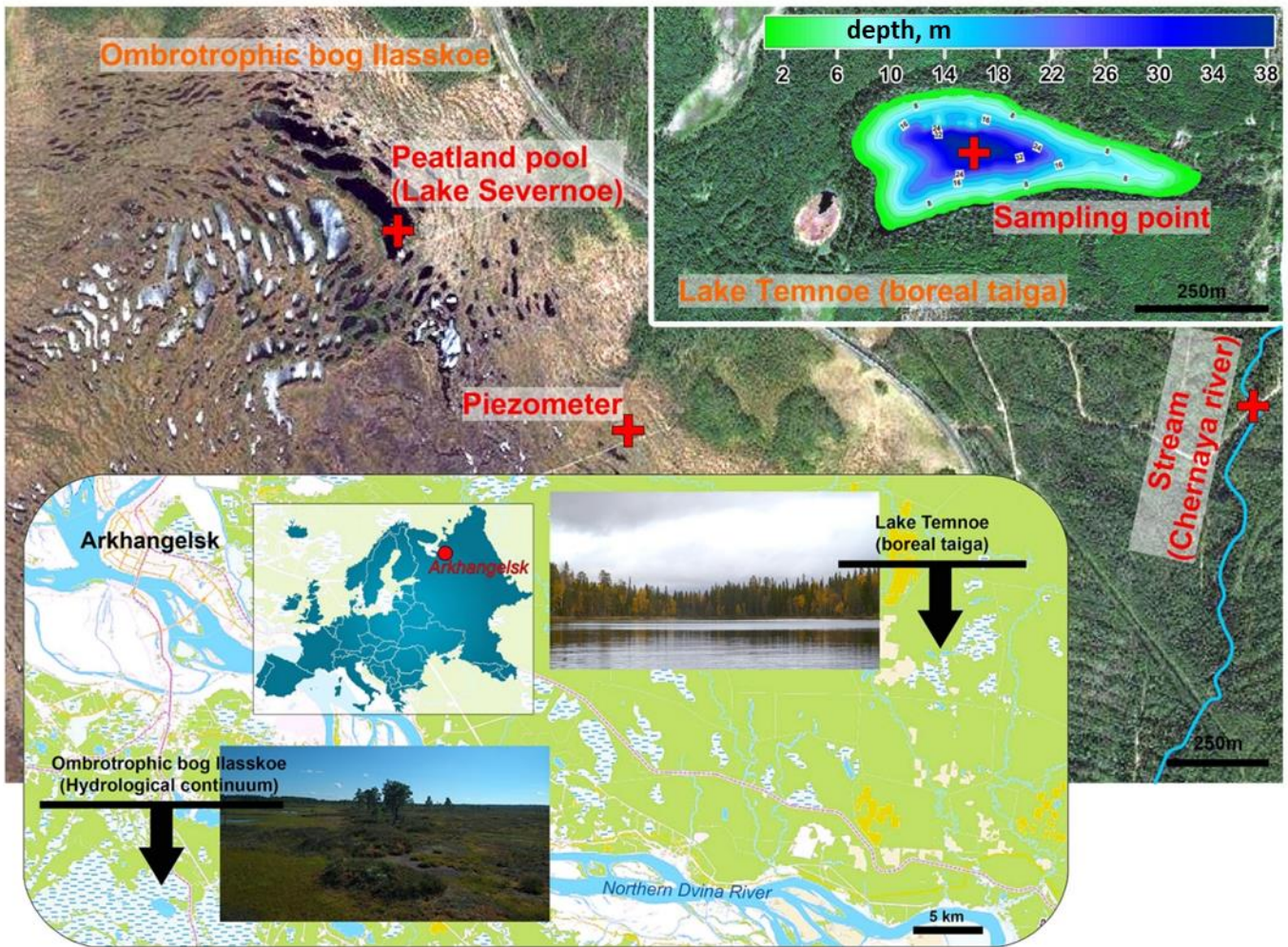
1077

1078

Fig. 1. Geographical location of studied hydrological continuum for Ilasskoe Bog waters and
deep stratified Lake Temnoe in the boreal forest. Photo and map credits of Chupakov A.V.

1081

1082

1083

1084

1085
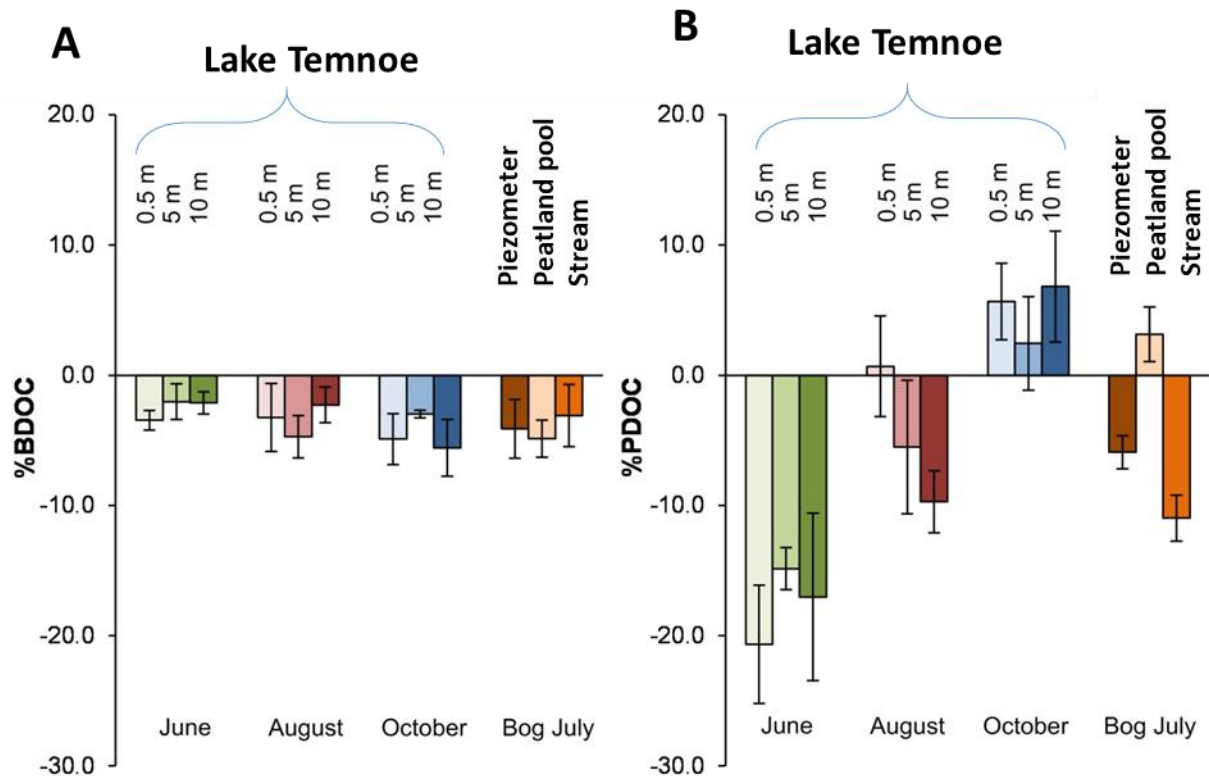
Fig. 2. Percentage of bio- (A) and photo- (B) degradable DOC presented as relative decrease in DOC concentration between the initial and final value for the Temnoe Lake (June, August and October) and Ilasskoe Bog surface waters (July). Error bars are 1 s.d. of duplicates relative to the control (see Eqn. 1-2 in the text). In accord with unified protocol of biodegradation experiments (Vonk et al., 2015), positive values signify nil photodegradation (experimental artifacts of DOC production).

1107

1108

1109

1110
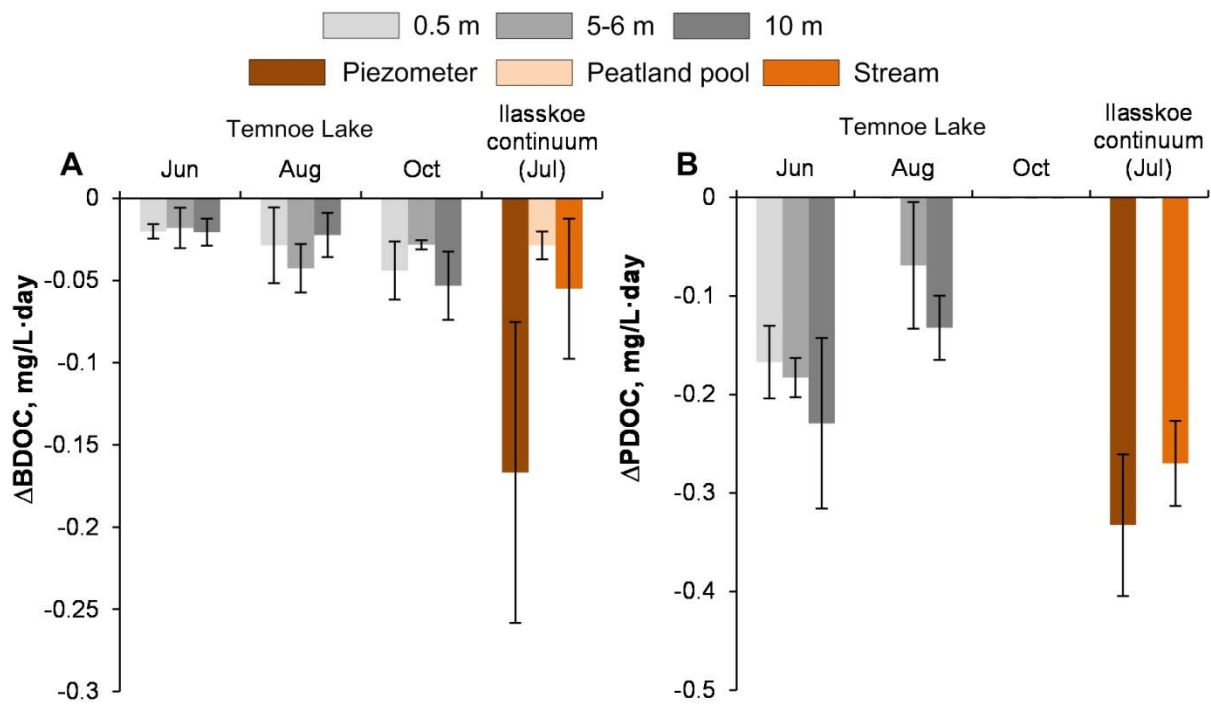
1111

1112

1113

1114   **Fig. 3.** Rates of DOC bio- (A) and photo- (B) degradation. The values are negative because

1115   they represent a decrease in DOC concentration over the course of the experiment.

1116

1117

1118

1119
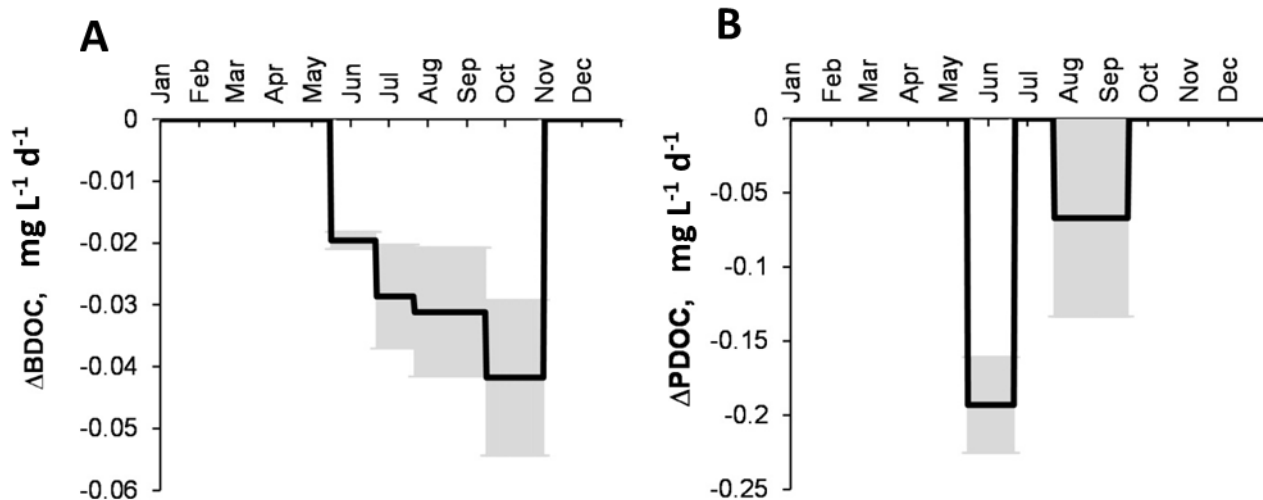
Fig. 4. Integral rates of bio- (ΔBDOC, **A**) and photo- (ΔPDOC, **B**) degradation in the 0-10 m layer of Lake Temnoe across the entire open-water period (May to October). Rate values are negative because they signify a decrease in DOC concentration. Note that there was no sampling from December to April and the photodegradation was not studied in July. Uncertainties are represented by gray shaded rectangles.
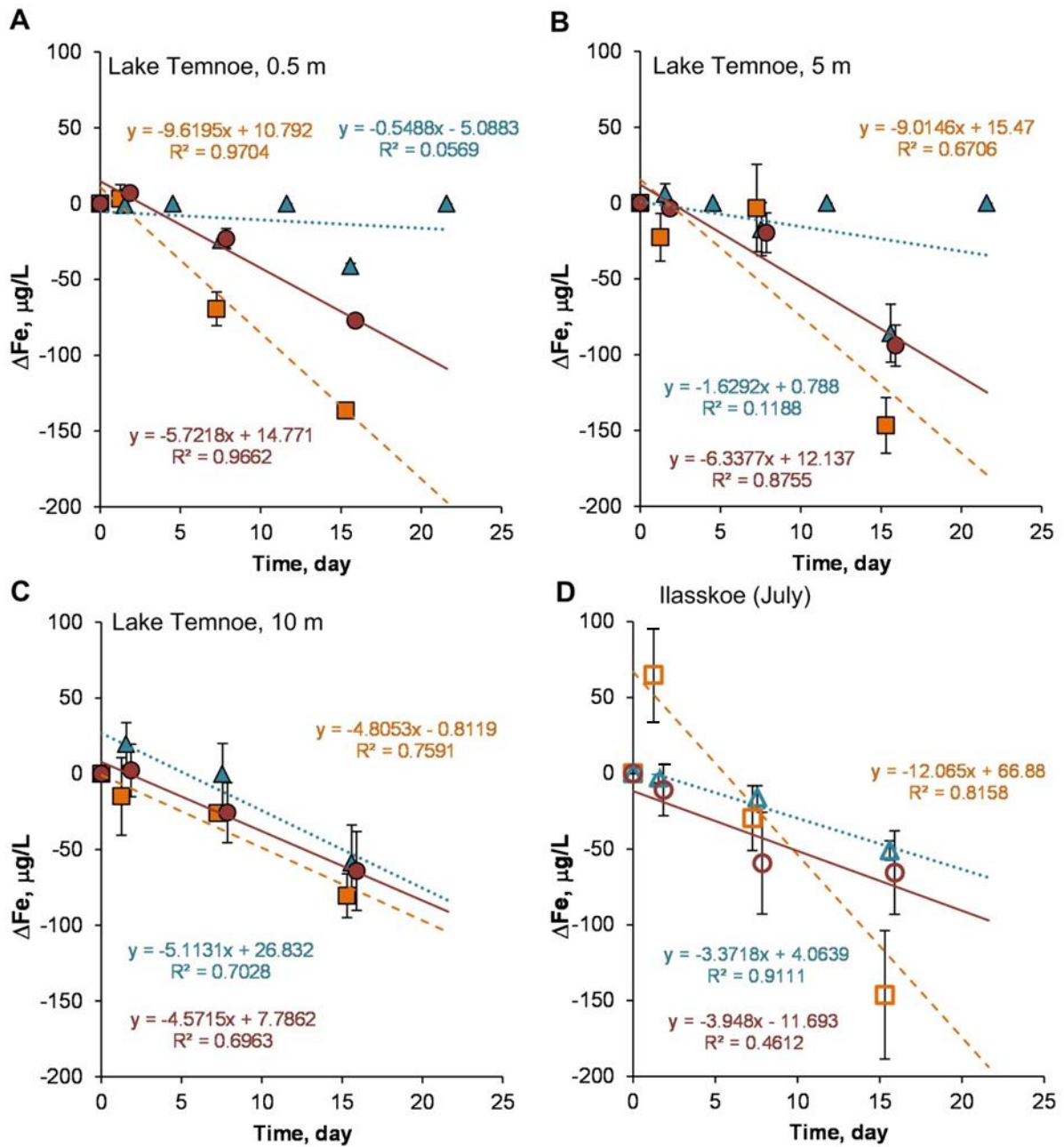
Fig. 5. Change in Fe concentration (relative to control) over time in biodegradation experiments. Error bars are 1 s.d. of duplicates. Temnoe Lake 0.5 m (A), 5 m (B) and 10 m (C) in June (squares), August (triangles) and October (circles). Ilasskoe Bog continuum in July (D) including piezometer (squares), Severnoe peatland pool (triangles) and stream Chernyi (circles).
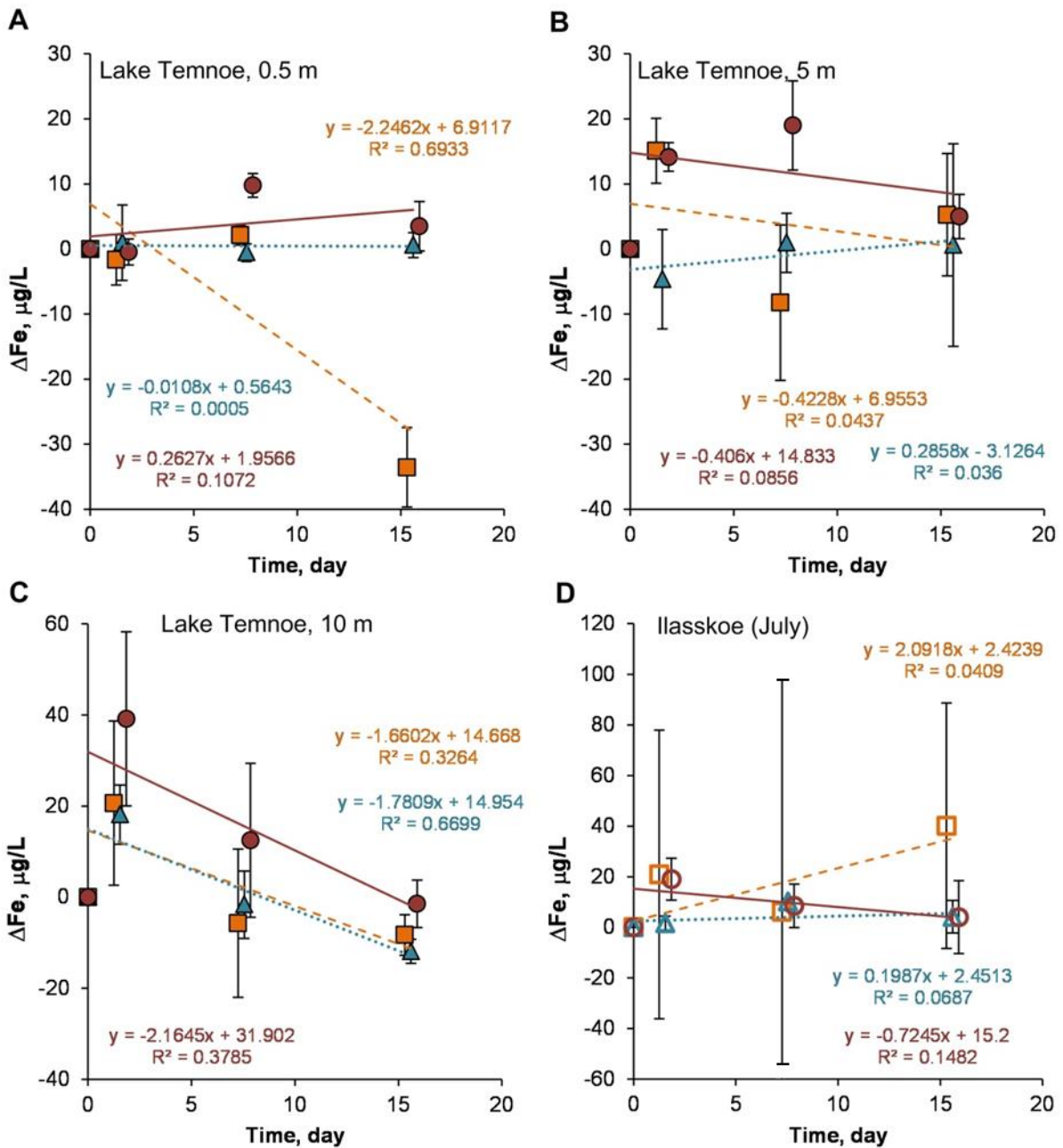
Fig. 6. Change in Fe concentration (relative to the control) over time in photo-degradation experiments. The error bars are 1 s.d. of duplicates. Lake Temnoe 0.5 m (A), 5 m (B) and 10 m (C) in June (squares), August (triangles) and October (circles). Ilasskoe continuum in July (D) includes piezometer (squares), peatland pool Severnoe (triangles) and stream Chernyi (circles)

1160 **Table 1.** Landscape setting, hydrochemical characteristics and CO_2 concentration and emission
1161 flux of studied waters. S.C. is specific conductivity and EB and OB is eutrophic and
1162 oligotrophic bacteria count, respectively.
1163 **1A.** Ilasskoe bog continuum in July.
1164

	Piezometer	Lake Severnoe	Stream Chernyi
GPS coordinates	N64.328694° E40.612556°	N64.334361° E40.609667°	N64.330982° E40.653352°
Description	Shallow groundwater	Peatland pool	Outlet stream
T,°C	11.4	19.4	13
O_2, mg/L	0.6	8.6	7.5
pH	3.9	4.0	5.7
S.C., $\mu S\ cm^{-1}$	46	17	26
DOC, mg L^{-1}	87.6	12.7	38.4
DIC, mg L^{-1}	0.32	0.40	0.38
$SUVA_{254}$	4.13	3.80	4.85
$P-PO_4$, $\mu g\ L^{-1}$	8.6	3.0	1.7
P_{total}, $\mu g\ L^{-1}$	153	10	20
$N-NO_3$, $\mu g\ L^{-1}$	111	70	98
$N-NH_4$, $\mu g\ L^{-1}$	85.4	16.1	12.6
N_{total}, $\mu g\ L^{-1}$	1180	222	399
Si, $\mu g\ L^{-1}$	1808	47	2076
CO_2, $\mu mol/L$	3360	55	318
CO_2 flux, mmol $m^{-2}\ d^{-1}$	1600	22	151
EB, CFU mL^{-1}	49360	56600	9000
OB, CFU mL^{-1}	54560	37900	21600

1165
1166 **1B.** Lake Temnoe across seasons and depths.
1167
1168

Month	Jun	Jun	Jun	Aug	Aug	Aug	Oct	Oct	Oct
	0.5	5	10	0.5	5	10	0.5	6	10
GPS	N64.47683° E041.74533°								
Description	Lake in the northern taiga								
T,°C	12.7	4,9	4,5	18.4	5.5	4.3	9.0	5.8	4.4
O_2, mg/L	8,45	4,8	4,5	7.78	4.93	2.63	8.90	4.46	2.14
pH	5.2	5.2	5.3	6.0	5.5	5.7	5.2	5.2	5.1
S.C., $\mu S\ cm^{-1}$	17	17	19	17	17	19	18	18	20
DOC, mg L^{-1}	12.6	19.2	21	19	19.5	21.2	19.4	20.6	20.6
DIC, mg L^{-1}	0.55	0.53	0.49	0.70	0.71	0.66	0.67	0.67	0.64
$SUVA_{254}$	4.6	4.7	4.6	4.2	4.5	4.5	4.3	4.3	4.7
$P-PO_4$, $\mu g\ L^{-1}$	2.9	3.3	6.4	0.9	3.6	9.4	3.8	4.6	4.2
P_{total}, $\mu g\ L^{-1}$	19	17	19	20	16	20	18	19	20
$N-NO_3$, $\mu g\ L^{-1}$	119	150	137	86	152	254	88	85	100
$N-NH_4$, $\mu g\ L^{-1}$	7.1	8.0	10.0	9.1	17.5	13.8	16.4	14.1	15.5
N_{total}, $\mu g\ L^{-1}$	305	420	408	355	315	337	425	416	396
Si, $\mu g\ L^{-1}$	1940	2268	2354	1183	2208	2714	2269	2380	2380
CO_2, $\mu mol/L$	99	309	329	110	256	337	223	232	253
CO_2 flux, mmol $m^{-2}\ d^{-1}$	32	-	-	46	-	-	71	-	-
EB, CFU mL^{-1}	-	36	50	259	92	270	780	220	105
OB, CFU mL^{-1}	50	570	420	-	190	-	680	150	66

1169

Table 2. The % bio- and photodegradable solutes (mean ± s.d.) whose relative change (concentration decrease) in the course of experiment was superior to that of SD. Prefix ΔB and ΔP represents the effect of bio- and photodegradation, respectively. Duration of biodegradation and photodegradation is 21.6±0.1 and 15.6±0.1 days, respectively. W represents the probability of measurable effect, significantly different from changes in the control reactors. Only the components with W ≥ 33% are presented. Temnoe Lake is deep stratified lake in the forest. Peizometer, peatland pool and outlet stream represent the hydrological continuum of the Ilasskoe Bog.

Index	Temnoe Lake 0.5 m (Jun)	Temnoe Lake 5 m (Jun)	Temnoe Lake 10 m (Jun)	Temnoe Lake 0.5 m (Aug)	Temnoe Lake 5 m (Aug)	Temnoe Lake 10 m (Aug)	Temnoe Lake 0.5 m (Oct)	Temnoe Lake 6 m (Oct)	Temnoe Lake 10 m (Oct)	Piezo-meter (Jul)	Peatland pool (Jul)	Outlet stream (Jul)
æ, µS/cm	17	17	19	17	17	19	18	18	20	46	17	26
ΔB(æ ±SD)	-24±4	-26±7	-30±5	-23±3	-27±3	-33±16	-24±7	-23±4	-17±5	0	-18±10	-29±4
DOC, mg/L	12.6	19.2	21.0	19.0	19.5	21.2	19.4	20.6	20.6	87.6	12.7	38.4
ΔB(DOC±SD)	3.4±0.8	2.0±1.4	2.1±0.8	3.2±2.6	4.7±1.6	2.3±1.4	4.9±2.0	3.0±0.3	5.6±2.2	4.1±2.3	4.9±1.4	3.1±2.4
ΔP(DOC±SD)	20.7±4.6	14.9±1.6	17.0±6.4	0	5.5±5.1	9.7±2.4	0	0	0	5.9±1.3	0	11.0±1.8
Al, µg/L	275	298	329	254	296	335	275	288	323	276	59	388
ΔB(Al±SD)	3.5±1.4	1.8±0.9	0	2.0±1.3	0	1.4±1.5	2.0±1.9	0	0	0.9±2.2	0	1.3±1.8
ΔP(Al±SD)	1.9±1.1	2.7±0.9	3.6±1.3	0	2.5±1.3	1.7±2.0	0.7±0.9	0	0	0	0	0.8±0.9
Ti, µg/L	1.5	2.1	2.6	1.1	2.0	2.6	1.7	1.9	2.5	3.7	0.6	5.0
ΔB(Ti±SD)	-9.2±1.6	-9.9±7.4	-2.6±2.7	-4.8±3.4	-1.8±2.7	0	-3.6±1.7	-1.0±3.1	-1.0±3.9	-2.3±3.6	-2.2±1.7	-1.4±2.2
ΔP(Ti±SD)	-0.1±3	-3±3	-8±3	0±0	-9±1	-3±2	-2±4	0	0	0	-20±4	-3.3±0.5
V, µg/L	0.5	0.6	0.7	0.4	0.5	0.7	0.4	0.5	0.7	1.1	0.5	1.3
ΔB(V±SD)	-8.3±16.2	-5.4±3.2	-4.9±2.3	-6.8±7.5	-10.0±4.6	-1.7±1.6	-14.7±11	-13.9±4.3	-16.1±1.7	-3.2±2.6	-0.2±3.4	-17.9±5.0
Mn, µg/L	39	55	79	17	48	93	30	47	105	78	9	47
ΔB(Mn±SD)	0	0	-0.3±2.2	-31.8±1.3	-3.2±1.6	-0.6±2.2	-4.8±2.2	-3.2±1.7	-0.4±0.1	0	0	-1.6±2.8
Fe, µg/L	358	527	710	165	460	795	317	448	820	4402	157	1006
ΔB(Fe±SD)	-18.1±2.5	-9.1±2.6	-5.4±1.6	-13.5±1.0	-6.3±2.6	-1.4±1.9	-9.5±1.4	-7.8±1.9	-3.3±1.8	-0.8±0.8	-13.6±4.3	-4.5±2.4
ΔP(Fe±SD)	-3.9±0.6	-2.0±1.9	-4.0±1.3	0	-2.9±1.5	-0.2±0.6	-1.2±0.4	0	0	0	0	0

1170

Table 2, continued.

Index	Temnoe Lake 0.5 m (Jun)	Temnoe Lake 5 m (Jun)	Temnoe Lake 10 m (Jun)	Temnoe Lake 0.5 m (Aug)	Temnoe Lake 5 m (Aug)	Temnoe Lake 10 m (Aug)	Temnoe Lake 0.5 m (Oct)	Temnoe Lake 6 m (Oct)	Temnoe Lake 10 m (Oct)	Piezo-meter (Jul)	Peatland pool (Jul)	Outlet stream (Jul)
Co, µg/L	0.28	0.39	0.68	0.07	0.30	0.65	0.18	0.31	0.74	0.45	0.06	0.30
ΔB(Co±SD)	-2.2±5.1	-1.2±2.1	-3.7±4.6	-32.7±2.6	-8.1±5.6	-2.7±3.3	-11.0±4.4	-9.1±5.1	-1.6±0.4	0	0	-20.6±27.8
Cu, µg/L	0.5	0.6	0.7	0.6	0.6	0.7	0.7	0.7	0.5	1.5	0.3	0.8
ΔB(Cu±SD)	0	0	0	-14.3±1.4	-6.8±4.0	-17.9±11.0	-5.3±4.8	-4.1±8.0	-1.4±12.3	0	-7.7±9.9	0
Ga, µg/L	0.017	0.022	0.026	0.012	0.016	0.023	0.017	0.015	0.024	0.126	0.016	0.066
ΔP(Ga±SD)	-14±6	-13±5	-10±4	0	-1±8	0	-10±4	0	0	-7±5	-5±8	-6±3
Y, µg/L	0.22	0.25	0.28	0.20	0.24	0.28	0.22	0.23	0.28	0.10	0.01	0.21
ΔP(Y±SD)	-1.3±4.6	-6.7±0.9	-5.3±2.5	0	-2.3±0.7	-1.0±1.6	-1.4±0.2	0	0	0	-5.8±2.7	0
Zr, µg/L	0.4	0.4	0.5	0.4	0.5	0.5	0.4	0.4	0.5	0.3	0.1	0.4
ΔP(Zr±SD)	-15±4	-14±0	-13±2	-9±20	-17±1	-14±3	-4±4	0	0	0	-32±3	-8±1
Nb, µg/L	0.016	0.020	0.025	0.012	0.020	0.024	0.017	0.018	0.025	0.033	0.005	0.042
ΔB(Nb±SD)	-3.6±10.2	-1.7±7.0	0	-7.7±4.8	-1.1±2.6	0	-7.3±2.3	-1.5±6.3	-5.0±4.0	-2.4±1.5	0	0
ΔP(Nb±SD)	-9±3	-8±3	-9±1	-6±23	-13±2	-10±5	-8±4	0	-3±3	0	-13±10	-10±4
Ba, µg/L	4.8	5.1	5.8	4.6	5.0	5.7	4.9	4.8	5.6	54.4	1.5	56.8
ΔB(Ba±SD)	-2.2±0.7	-2.8±1.7	-1.0±2.7	0	0	0	-1.9±0.5	-1.7±3.7	-5.9±1.6	0	0	-1.3±3.4
La, µg/L	0.23	0.26	0.30	0.21	0.26	0.32	0.24	0.27	0.31	0.07	0.01	0.22
ΔB(La±SD)	-4.9±6.5	0	0	-3.9±0.9	-0.3±1.6	-2.6±1.5	-1.1±3.6	-2.4±1.2	-4.0±2.8	-0.8±10.4	-29.7±10.0	-2.0±2.8
ΔP(La±SD)	-3.8±3.6	-1.2±5.9	-2.0±2.7	0	-3.6±1.0	-3.2±1.6	-1.8±0.9	-2.6±1.0	0	0	-13.5±3.0	0
Ce, µg/L	0.58	0.65	0.71	0.50	0.62	0.78	0.59	0.63	0.78	0.21	0.03	0.56
ΔB(Ce±SD)	-5.2±4.2	0	0	-4.4±0.7	-0.1±1.4	-0.8±1.0	-0.9±2.9	-0.8±1.1	-2.2±2.2	0	-9.3±5.9	-2.0±1.9
ΔP(Ce±SD)	-4.9±1.9	-6.2±1.2	-1.1±1.7	0	-1.5±0.5	-3.2±1.7	-1.9±1.2	0	-0.047±0.46	-3.7±1.5	-2.4±1.6	-3.6±1.1

Table 2, continued.

Index	Temnoe Lake 0.5 m (Jun)	Temnoe Lake 5 m (Jun)	Temnoe Lake 10 m (Jun)	Temnoe Lake 0.5 m (Aug)	Temnoe Lake 5 m (Aug)	Temnoe Lake 10 m (Aug)	Temnoe Lake 0.5 m (Oct)	Temnoe Lake 6 m (Oct)	Temnoe Lake 10 m (Oct)	Piezo-meter (Jul)	Peatland pool (Jul)	Outlet stream (Jul)
Pr, µg/L	0.075	0.085	0.094	0.069	0.082	0.105	0.077	0.084	0.102	0.027	0.005	0.070
ΔB(Pr±SD)	-1.9±5.2	0	0	-4.0±1.1	0	-0.7±1.3	0	-0.9±1.6	-3.2±2.3	-3.0±1.7	-10.8±8.4	-1.7±2.3
ΔP(Pr±SD)	-3.0±3.9	-5.5±0.9	-0.4±2.9	13.7±20.8	0	-6.1±2.8	0	-1.3±1.8	0	-0.01±2.4	-16.9±3.0	-2.4±2.1
Nd, µg/L	0.33	0.34	0.39	0.29	0.33	0.42	0.33	0.32	0.41	0.11	0.02	0.27
ΔP(Nd±SD)	-7.8±2.4	-4.5±2.5	-0.8±2.1	0	0	-3.8±2.5	-2.0±3.3	0	0	-2.5±2.8	-24.7±6.2	0
Eu, µg/L	0.015	0.017	0.016	0.012	0.016	0.020	0.014	0.018	0.021	0.011	0.001	0.017
ΔP(Eu±SD)	0	-10.9±3.3	0	0	-0.8±4.7	-3.0±4.0	0	-8.7±8.4	-6.9±4.2	-23.7±8.6	-58.2±15.2	-1.0±1.0
Gd, µg/L	0.06	0.07	0.08	0.05	0.07	0.08	0.06	0.07	0.09	0.02	0.00	0.06
ΔP(Gd±SD)	-0.2±4.4	-6.5±2.9	-3.5±3.5	0	-6.0±3.2	-7.6±1.9	-2.3±2.0	0	-6.7±3.2	0	0	-3.2±3.5
Ho, µg/L	0.009	0.009	0.011	0.007	0.009	0.011	0.009	0.009	0.011	0.004	0.0004	0.009
ΔP(Ho±SD)	-1.9±1.5	-0.3±1.6	-4.6±6.5	0	-0.1±3.6	-3.4±3.2	-11.0±4.9	0	0	-21.5±11.3	0	-10.9±5.5
Er, µg/L	0.023	0.025	0.033	0.022	0.026	0.030	0.022	0.023	0.031	0.011	0.001	0.023
ΔB(Er±SD)	0	0	0	-5.2±3.0	-2.1±1.8	0	-2.1±3.5	0	-2.0±5.3	-15.6±4.9	-22.9±19.5	0
Pb, µg/L	0.23	0.24	0.23	0.16	0.23	0.39	0.28	0.28	0.32	11	0.35	0.65
ΔB(Pb±SD)	0	0	0	-21.3±2.5	-2.0±7.6	-2.4±1.6	-8.2±3.3	-7.2±9.9	-0.8±2.7	0	-17.4±1.0	-8.5±10.9
Th, µg/L	0.046	0.052	0.066	0.058	0.054	0.064	0.053	0.054	0.061	0.019	0.005	0.050
ΔP(Th±SD)	0	0	-11.6±2.6	-12.2±22.5	-7.8±3.2	-18.1±5.6	0	0	-2.0±1.9	0	-49.5±1.3	-10.6±0.8

1177
1178
1179 **Table 3.** Mean (±SD), depth-integrated rates of bio- and photodegradation (mg C L^{-1}d^{-1})
1180
1181

	$V_{\text{Biodegradation}}$	$V_{\text{Photodegradation}}$
Object		
Lake Temnoe		
Forest Lake (Jun)	-0.02±0.0014	-0.19±0.03
Forest Lake (Aug)	-0.031±0.010	-0.067±0.066
Forest Lake (Oct)	-0.042±0.013	0
Ilasskoe Bog continuum (July)		
Piezometer water	-0.17±0.09	-0.33±0.07
Peatland pool	-0.029±0.008	0
Outlet stream (Chernyi)	-0.055±0.043	-0.27±0.043

1182

1183

1184

1185

1186

1187

1188

1189

1190